Eur. Phys. J. A **18**, 605–626 (2003)
DOI 10.1140/epja/i2002-10167-8

THE EUROPEAN PHYSICAL JOURNAL A

Properties of ^{152}Gd collective states

J. Adam[1,a], J. Dobeš[2], M. Honusek[2], V.G. Kalinnikov[1], J. Mrázek[2], V.S. Pronskikh[1,b], P. Čaloun[1,a], N.A. Lebedev[1], V.I. Stegailov[1], and V.M. Tsoupko-Sitnikov[1]

[1] Joint Institute for Nuclear Research, Dubna, Russia
[2] Nuclear Physics Institute ASCR, CZ-25068 Řež, Czech Republic

Received: 21 May 2002 / Revised version: 26 May 2003 /
Published online: 18 November 2003 –
Communicated by D. Schwalm

Abstract. The decays of ^{152}Tb ($T_{1/2}$ = 17.5 h) and ^{152}Gd excited states have been investigated by the analysis of γ-rays and $\gamma\gamma$-coincidences measured with the use of high-resolution HPGe detectors. The source of ^{152}Tb was prepared by chromatographic isolation followed by electromagnetic separation from a tantalum target irradiated by an internal proton beam of the LNP JINR phasotron. New and more precise data on the γ-transitions and excited states of ^{152}Gd are reported. Using previously published data on internal-conversion electrons many transition multipolarities are suggested, some of them with $E0$ admixture. The EC/β^+ ratio was found for a number of low-lying levels, for most of the levels their spins, parities, and $\log ft$ are given. The excited levels of ^{152}Gd were deduced from the analysis of $\gamma\gamma$-coincidences. The experimental level energies and reduced transition probabilities are compared with the calculations by phenomenological formulae as well as in the frameworks of theoretical models.

PACS. 29.30.Kv X- and gamma-ray spectroscopy – 23.20.-g Electromagnetic transitions – 21.10.-k Properties of nuclei; nuclear energy levels – 21.60.-n Nuclear structure models and methods

1 Introduction

The even-even stable nucleus $^{152}_{64}$Gd$_{88}$ ($I^\pi = 0^+$) is located at the limits of the region of nuclear deformation; consequently, the origin of its excited states may refer to that of either spherical or weakly deformed nuclei as well as its wave function may be presented as a mixed state of these two types. One can also expect the nuclei belonging to the transitional region (between spherical and deformed ones) to exhibit an $E0$ multipolarity admixture to $M1(E2)$ transitions between the levels of identical non-zero spin.

The results of experimental investigations of the ^{152}Gd excited states published up to 1995 were compiled and evaluated by A. Artna-Cohen [1]. They were based on the measurements of ^{152}Eu ($I^\pi = 3^-$, $T_{1/2}$ = 13.5374 y) β^- decay by R.A. Meyer [2], N.M. Stewart *et al.* [3], and J. Goswamy *et al.* [4], and also on the decay of the isomeric state ^{152m}Eu ($I^\pi = 0^-$, $T_{1/2}$ = 9.3116 h) by K.P. Artamonova *et al.* [5]. The EC/β^+ decay of ^{152}Tb ($I^\pi = 2^-$ $T_{1/2}$ = 17.5 h) and the ^{152}Gd excited states were studied by D.R. Zolnowski *et al.* [6], J. Adam *et al.* [7], and I. Tago *et al.* [8]; the decay of the isomer ^{152m}Tb ($I^\pi = 8^+$ $T_{1/2}$ = 4.2 min) was measured by D.R. Zolnowski *et al.* [9]. The angular distribution of the γ-quanta emitted from the oriented nuclei ^{152}Tb was investigated by P.O. Lipas *et al.* [10]. Excited levels of the ^{152}Gd nucleus were studied in the reactions $(\alpha, 4n\gamma)$ (D.R. Zolnowski *et al.* [9] and M. Guttormsen *et al.* [11]), and $(p, 2n\gamma)$ (Y. Gono [12]).

Lifetimes of several ^{152}Gd states were measured in the Coulomb excitation by N.R. Johnson *et al.* [13]. In the work of D.R. Fleming *et al.* [14] the reaction ^{154}Gd(p,t) ^{152}Gd was studied. R. Bloch *et al.* [15] analyzed the results of inelastic scattering of deuterons on ^{152}Gd.

During the last seven years, the $\gamma\gamma$ angular correlations in the ^{152}Eu decay have been measured by M. Asai *et al.* [16] and the magnetic moment of 2^+_1 and 4^+_1 by the transient magnetic-field technique by N.A. Matt *et al.* [17]. Nuclear moments and isotope shifts were deduced by K. Blaum *et al.* [18] by means of the resonance ionization mass spectrometry.

A large number of works was also dedicated to the calculations of the quantum characteristics of the ^{152}Gd levels, the Interacting Boson Model was used in [19–38], the dynamic deformation model in [39–43], and the relativistic mean-field theory in [44–49]. Some results of these calculations are discussed further in more detail.

[a] On leave from Nuclear Physics Institute of ASCR, Řež, Czech Republic.
[b] On leave from Saint Petersburg State Institute of Technology, Russia; e-mail: Vitali.Pronskikh@jinr.ru

The properties of the excited levels with energies up to 1500–2000 keV have been studied quite well whereas the experimental data for the higher-energy levels are not so complete. Rather detailed data on the intensities of internal-conversion electron transitions in this decay were previously published in [7]. The latest results of the single γ-ray and $\gamma\gamma$-coincidence measurements were published in [6].

2 Experimental setup

A tantalum target was irradiated by an internal proton beam ($E_p = 660$ MeV, $I_p = 5$ μA) of the LNP phasotron and a radioactive source of ^{152}Tb was prepared from it by means of chromatographic isolation followed by electromagnetic separation.

Gamma-rays from the ^{152}Tb decay were measured in the energy range from 5 keV to 1500 keV with a planar HPGe detector ($\varnothing$ 12 mm, thickness 5 mm) with the energy resolution $\Delta E_\gamma = 350$ eV for $E_\gamma = 6.9$ keV and with a coaxial HPGe detector CANBERRA ($\varepsilon = 19\%$ and $\Delta E_\gamma = 1.8$ keV (^{60}Co)). In measurements with the coaxial detector a 1 mm Cu + 1 mm Cd filter was used and the source-to-detector distance was $d = 80$ mm. In the higher-energy range (300–4000 keV), γ-quanta were recorded with another coaxial HPGe detector ORTEC ($\varepsilon = 28\%$, $\Delta E_\gamma = 1.9$ keV (^{60}Co)). In the latter measurements a 1 mm Cu + 2 mm Cd + 7 mm Pb filter was mounted on the detector and the source-to-detector distance was set to 10 mm. The assignment of gamma-peaks to the ^{152}Tb decay was based on their intensity fall with time, the background peaks and the peaks from other Tb isotopes were taken into consideration. Gamma-quanta from the neighboring isotopes ^{151,153,154}Tb were also observed in the spectra. Their activity contributed from 10^{-3} to 10^{-5} of the ^{152}Tb activity.

The $\gamma\gamma$-coincidences were recorded by the two HPGe detectors CANBERRA and ORTEC described above. The axes of the detectors made an angle of $\approx 100^\circ$ and the source-to-detector distance was ≈ 35 mm. The detectors were protected with a 7 mm thick Pb filter placed between them to avoid registration of Compton-scattered photons. The resolution time of the coincidence circuit was ≈ 20 ns. The coincidences were recorded event by event as the channel numbers K_i and K_j in the first and second detectors, respectively, and also K_q —the time passed between the detection of these two pulses in the interval (0 ns–180 ns).

3 Analysis of single γ-rays

Transition energies in the ^{152}Tb decay were determined by the "internal calibration" approach: the ^{152}Tb source and a standard source of nearly equal intensities were placed at the same strictly defined distance of 10 mm from the detector. The γ-radiation was recorded in a broad energy range with a multichannel analyzer SPECTRUM MASTER 919 (ORTEC) as 16384-channel spectra. The spectra were handled by the computer code DEIMOS [50], the initial parameters of the fit were chosen interactively. A slight non-Gaussian variation in the shape of the high-intensity peaks was taken into account by insertion of an additional peak into the left slope of the main one.

The energies of ^{56}Co, ^{57}Co, ^{133}Ba, ^{152}Eu and ^{154}Eu γ-lines for calibration purposes were taken from [51], while those of ^{226}Ra from [52]. A 2nd-power polynomial was used for the calibration. The main part of the ^{152}Gd excited-level scheme was built on 86 transitions that had been observed in $\gamma\gamma$-coincidences [6], while 5 of these γ-rays were doublet γ-rays close in energy. The remaining 81 transitions were placed within 43 levels, and the energies of the levels were determined by least-squares fitting. We obtained $\chi^2 = 1.19$ for a set of 77 transitions, which can prove the correctness of the E_γ and ΔE_γ determination. We also unambiguously placed 87 more transitions within 45 levels using the energy balance condition

$$\left[(E_i - E_k)_{(\mathrm{lev})} - E_\gamma(k)_{(\mathrm{tr})}\right] \leq 2\sigma\,.$$

During the determination of the transitions' intensities a thorough analysis of ballast peaks, namely, sum peaks, single and double escape peaks, was done. Energies and intensities of those peaks were calculated with the programs described in [53]. In the γ-ray energy range from 900 keV to 4000 keV measured with a HPGe detector equipped with a thick filter, we observed 661 peaks, 62 of which were recognized as ballast and 331, identified as full-energy peaks, were corrected for a ballast admixture. In some cases these corrections were rather substantial. Note that intensities of the 1048.1, 1123.3, 1343, 1353 and 2966 keV transitions (see [6]) are completely equal to those of the ballast peaks. Substraction of a ballast peak intensity out of a full-energy peak's one introduced additional uncertainty in the energy of the latter peak.

4 Transition multipolarities

Relative intensities of internal-conversion electrons (ICE) from the K-shell were taken from [7] where the measurements of [54] had been completed and made more precise. The ICE measurements were carried out with an orange-type β-spectrometer ($\Delta H\rho/H\rho = 0.4\%$, $\varepsilon \approx 1\%$) in the low-energy range (below 1000 keV) and with a twofold double-focussing $2\pi\sqrt{2}$-type very low-background (< 1 count per day) spectrometer ($\Delta H\rho/H\rho = 0.21\%$, $\varepsilon \approx 0.1\%$) in the high-energy range (above 900 keV). The energy E_e (keV) and momentum ($H\rho$) of ICE are known to be connected by the relation

$$\frac{\Delta E_e}{E_e} = \left(1 + \frac{511}{511 + E_e}\right)\frac{\Delta H\rho}{H\rho}\,.$$

Thus, the resolution of the HPGe detectors is better than that of the β-spectrometers. That is why some of the conversion lines are considered as being complex (see below). On the basis of previous investigations of the ^{152}Tb decay scheme, some intense transitions were surely assigned either $E2$ or $E1$ multipolarities. The coefficient

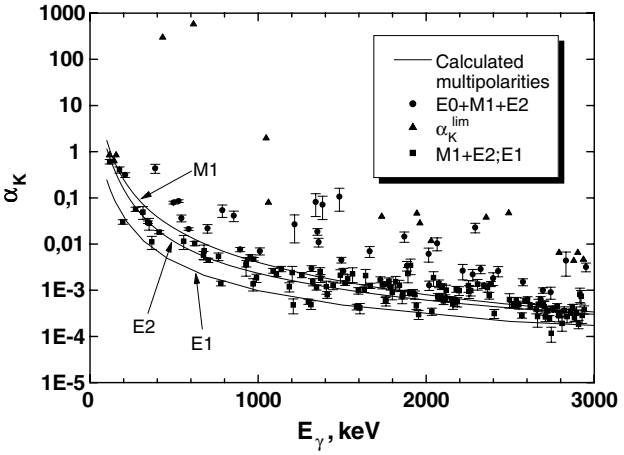

Fig. 1. Comparison of $\alpha_K^{\rm exp}(E_i)$ $\alpha_K^{\rm theo}(E_i, XL)$, $XL = M1$, $E1$, $E2$.

k, needed to connect I_K and I_γ internal units, was determined separately in both the low-energy region, using the 344 ($E2$), 411 ($E2$) and 778 keV ($E1$) ($k = 0.101(4)$) transitions, and the high-energy one (> 900 keV), using the 970($E1$), 990($E2$), 1185($E2$), 1209($E1$), 1299($E1$), 1314($E1$), 1941($E2$), 2033($E1$) and 2113 keV ($E2$) ($k = 0.086(7)$). We determined this k by comparison of the experimental and theoretical K-shell conversion coefficients (α_K), *i.e.*, $k\frac{I_K(E_i)}{I_\gamma(E_i)} = \alpha_K^{\rm theo}(E_i(XL))$, where XL are transition multipolarities. The theoretical $\alpha_K^{\rm theo}$ ($E_i(XL)$) were received by square interpolation of the tabulated data [55] to the required energies with use of the computer code [56]. Having calculated k, we used our measurements of I_γ and I_K taken from [7] to calculate $\alpha_K^{\rm exp}(E_i)$ and transition multipolarities, see table 3 below and fig. 1. Multipolarities of some double (triple) transitions were also determined. To extract multipolarity information from the measured intensities, a compilation was made based upon the measured gamma-ray intensities and theoretical K-shell conversion coefficients. We calculated K-electron internal-conversion intensities for various multipolarity characters for the doublet (triplet) transitions. The total K-ICE intensity for each doublet (triplet) was then compared to the measured I_K values. Sums that coincide with measured values within experimental uncertainties determined the possible multipolarities of doublets (triplets), see table 1 in ref. [57] for more details.

For a number of transitions $\alpha_K^{\rm exp}$ exceeded $\alpha_K^{\rm theo}(M1)$, which can be explained by $E0$ or $E0 + M1$ multipolarities of those transitions. The transitions with $M2$ multipolarities are less probable due to their insignificant reduced probabilities $B(M2)$. The $M1$ multipolarities were assigned tentatively but those transitions might have an $E0$ or $M1{+}E2$ admixture as well. Establishing such a multipolarity would require more sophisticated experiments, *e.g.* studies of the angular distribution of γ-quanta emitted from oriented nuclei or $\gamma\gamma$ angular correlations. For most of the transitions, the $E0$ admixtures were determined for the first time. The determination of $E0$ and $M1 + E0$ multipolarities is based on the correct calculation of the intensity K-conversion electrons. For a number of K-conversion lines their intensities could turn out to be too high, provided there exist overlaps of those lines with L-, M-, and N-conversion lines from other transitions. We calculated the maximum $I_L + I_M + I_N$ intensities (in accordance with possible multipolarities) for the transitions that were known before. For the transitions which we observed for the first time (I_γ is given with its uncertainty) as well as for the transitions that were not observed, we determined only upper limits to their I_γ. On the basis of our analysis, we can conclude that for the transitions with energies higher than 400 keV, such corrections for overlapping of $L + M + N$ conversion electrons belonging to new and possible transitions are negligible.

The $E0$ admixture is supposed to be proved if the following equation is satisfied:

$$\alpha_K^{\rm exp} - 3\sigma(\alpha_K^{\rm exp}) > \alpha_K^{\rm theo}(M1)\,.$$

We have found that nine ($M1 + E0$) transitions obey the above equation. We surmise that transitions meeting a weaker condition,

$$\alpha_K^{\rm exp} - 2\sigma(\alpha_K^{\rm exp}) > \alpha_K^{\rm theo}(M1) > \alpha_K^{\rm exp} - 3\sigma(\alpha_K^{\rm exp}),$$

still may have $M1{+}E0$ multipolarity, and enclose them in parentheses. We observed 19 such transitions, 8 of which are doublet ones.

We calculated the gamma-ray intensity upper limits for even those transitions where only K-conversion coefficients had been known, and then estimated their $\alpha_K^{\rm exp}$ lower limits. Of these values, 11 meet the stronger equation above, while 7 more the weaker one. The multipolarities of these transitions may be either $E0$ or $M1 + E0$. As we have not observed the gamma-rays corresponding to the decay of ^{152}Tb for these latter transitions, the inexactness in the conclusion on their multipolarity becomes even greater.

The fundamental property of an $E0$ transition is its electron conversion probability $W_e(E0)$ ($e = K, L_1, \ldots$):

$$W_e(E0) = \rho^2(E0)\Omega_e\,.$$

ρ depends linearly on the matrix elements:

$$\rho(E0; i \to f) = \frac{\langle f|M(E0)|i\rangle}{eR^2}\,,$$

containing information on the nuclear structure. Ω_e, where ($e = K, L_1, \ldots$), is the electronic factor, which depends on the wave function overlapping between the electron and the nucleus, on the nuclear charge Z and on the transition energy. It does not depend on the nuclear structure [58, 59]. The main property of a monopole transition is its matrix element $\rho(E0)$. Its value can be extracted from the experimental data using the relation [60]:

$$\rho^2(E0; 0_i^+ \to 0_f^+) = \frac{I_K(E0; 0_i^+ \to 0_f^+)}{I_K(E2; 0_i^+ \to 2_j^+)} \times \frac{\alpha_K(E2; 0_i^+ \to 2_j^+)}{\Omega_K(E0; 0_i^+ \to 0_f^+)} W_\gamma(E2; 0_i^+ \to 2_j^+)\,,$$

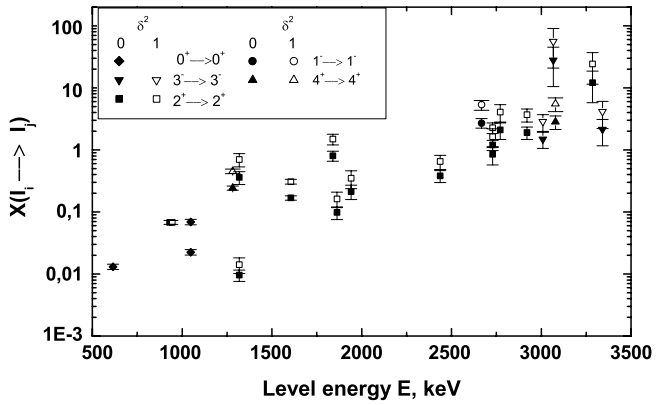

Fig. 2. Dependence of the Rasmussen parameters X on the energies of the initial levels that are de-excited by the given transitions.

where $W_\gamma(E2; 0_i^+ \to 2_j^+)$ is the absolute $E2$ probability of a transition between a 0_i^+ level and a lower 2_j^+ one:

$$W_\gamma(E2; 0_i^+ \to 2_j^+) = \frac{\ln 2}{T_{1/2}(0_i^+)_{(\mathrm{lev})}} \times \frac{I_\gamma(E2; 0_i^+ \to 2_j^+)}{\sum_{m=1}^{i-1} I_{im}^{\mathrm{tot}}},$$

where I_{im}^{tot} is the total intensity of transitions between level i and lower, $m = i-1, i-2, \ldots 1$, levels (1 marks the ground state). Unfortunately, only two lifetimes of excited states are known: 615 keV, 0^+, $T_{1/2} = 37(8)$ ps and 930 keV 2^+, $T_{1/2} = 7.3(6)$ ps [13], de-excited by $E0$ and $E0 + M1 + E2$ transitions, respectively. The $M1 + E2$ mixing parameter $\delta = -3.05(14)$ for the 586 keV transition was determined from the $\gamma\gamma(\Theta)$ angular-correlation measurements [61]. Using $T_{1/2}$, δ and the data of our measurements, we calculated:

$$\rho^2(930, 2^+ \to 344, 2^+) = 46(4) \times 10^{-3},$$

$$\rho^2(615, 0^+ \to 0, 0^+) = 66(14) \times 10^{-3}.$$

The latter ρ^2 is compared with the calculated one $\rho^2_{\mathrm{calc}} = 79 \times 10^{-3}$ [62], which refers to the maximum mixture of spherical and deformed state wave functions ($\beta_{\mathrm{def.}} = 0.192$). The ratio of the matrix elements of the transitions between the lowest 0^+ levels is $\left|\frac{\rho_{1047}}{\rho_{432}}\right| = 0.169$. As for the other $E0$ and $M1 + E0$ transitions, only their reduced-probability ratios (Rasmussen parameters) could be determined because the data on their lifetimes were absent:

$$X = \frac{B(E0; 0_i^+ \to 0_j^+)}{B(E2; 0_i^+ \to 2_k^+)} \qquad \text{for transitions } \ 0^+ \to 0^+,$$

or

$$X = \frac{B(E0; I_i \to I_f)}{B(E2; I_i \to I_k)} \qquad \text{for transitions } \ I_i = I_f \neq 0.$$

One can calculate this parameter from the experimental data using the relation [60]

$$X = 2.56 \times 10^{-6} A^{4/3} \frac{E_\gamma^5(E2) I_K(E0)}{\Omega_K(E0) I_K(E2)} \alpha_K(E2).$$

As a rule, the multipolarity mixtures $E0 + M1 + E2$ were not known quantitatively, therefore, the parameters X_1 and X_2 were supposed to have either $E0 + M1$ (with $\delta^2 = 0$) or $E0 + M1 + E2$ (with $\delta^2 = 1$) multipolarities. X_1 and X_2 values *versus* level energies are given in fig. 2. One can observe their monotonous growing, which proves qualitative changes in the structure of the states with their increasing excitation energy.

5 Analysis of $\gamma\gamma$-coincidences and the decay scheme

True coincidences were selected by setting a time gate and sorting the raw data into a two-dimensional matrix. The spectra of $\gamma\gamma$-coincidences were obtained by setting gates on intensive γ-peaks followed by substraction of the Compton background spectra from the resulting ones. The number of events was increased by a factor of two by summing each pair of the gate spectra from the X and Y detectors corresponding to the same γ-energy. Before summing up, these spectra were corrected channel by channel for non-linearity of the detectors' electric circuits. The number of the $\gamma\gamma$-coincidences acquired in a spectrum by gating a peak with $E_{nj}(\gamma)$ for the X detector $S_{\gamma\gamma}^{\bar{X},Y}(E_{nj}(\gamma), E_{im}(\gamma))$ is

$$S_{\gamma\gamma}^{\bar{X},Y}(E_{nj}(\gamma), E_{im}(\gamma)) = \varepsilon_\gamma^X(E_{nj}(\gamma)) I_\gamma(E_{nj}(\gamma)) \times \varepsilon_\gamma^Y(E_{im}(\gamma)) I_\gamma(E_{im}(\gamma)) R_{ji} NTW(\Theta),$$

where indices n, j, i, m are the numbers of the excited states between which the transition occurs, N is the number of nuclei decayed per second, T is the coincidence measurement time, R_{ij} is the branching coefficient, $\varepsilon_\gamma^X, \varepsilon_\gamma^Y$ is the absolute recording efficiency of the X and Y detectors for γ-quanta with E_γ, $W(\Theta)$ is the angular-correlation coefficient of the coinciding γ-quanta. Analogously, for the Y detector we have:

$$S_{\gamma\gamma}^{X,\bar{Y}}(E_{im}(\gamma), E_{nj}(\gamma)) = \varepsilon_\gamma^Y(E_{nj}(\gamma)) I_\gamma(E_{nj}(\gamma)) \times \varepsilon_\gamma^X(E_{im}(\gamma)) I_\gamma(E_{im}(\gamma)) R_{ji} NTW(\Theta).$$

Thus, the total number of coincidence events gated in both detectors for a pair of coincident γ-quanta is

$$S_{\gamma\gamma}^{\bar{X},\bar{Y}}(E_{im}(\gamma), E_{nj}(\gamma)) = S_{\gamma\gamma}^{\bar{X},Y}(E_{nj}(\gamma), E_{im}(\gamma)) + S_{\gamma\gamma}^{X,\bar{Y}}(E_{im}(\gamma), E_{nj}(\gamma)).$$

Recording $\gamma\gamma$-coincidences we simultaneously recorded

single γ-spectra with the same two detectors. The number of γ-quanta recorded in the X and Y spectra is

$$S_\gamma^X(E_{nj}(\gamma)) = \varepsilon_\gamma^X(E_{nj}(\gamma))I_\gamma(E_{nj}(\gamma))NT$$

or

$$S_\gamma^Y(E_{nj}(\gamma)) = \varepsilon_\gamma^Y(E_{nj}(\gamma))I_\gamma(E_{nj}(\gamma))NT\,.$$

Using the above relations one can calculate the branching ratio from the experimental data:

$$(R_{ji})_{\rm exp} = \frac{S_{\gamma\gamma}^{\bar{X},\bar{Y}}(E_{im}(\gamma),E_{nj}(\gamma))\,[W(\Theta)NT]^{-1}}{S_\gamma^X(E_{nj}(\gamma))S_\gamma^Y(E_{im}(\gamma))+S_\gamma^X(E_{im}(\gamma))S_\gamma^Y(E_{nj}(\gamma))}. \quad (1)$$

We found it convenient to exclude the NT coefficient by considering the experimental branching coefficient ratio $(R_{ji}/R_{22})_{\rm exp}$ and comparing it to the calculated one $(R_{ji}/R_{22})_{\rm calc}$ which had been deduced from the proposed decay scheme and placement of the γ-transitions,

$$(R_{ji})_{\rm calc} = s_i D_{ji}\,, \quad (2)$$

$$\text{where} \qquad s_i = \frac{1}{\sum_{x=1}^{i-1} I_{ix}} \qquad \text{and} \qquad d_{ix} = s_i I_{ix}\,,$$

where I_{ix} is the total γ-transition intensity, and the branching coefficient D_{ji} is deduced from the relation

$$D_{ji} = d_{ji} + \sum_{z_1>i}^{j-1} d_{jz_1}d_{z_1i} + \sum_{z_{\eta-1}>z_{\eta-2}}^{j-1}\sum_{z_{\eta-2}>z_{\eta-3}}^{j-2} \cdots \sum_{z_1>i}^{j-(\eta-1)} d_{jz_{\eta-1}}d_{z_{\eta-1}z_{\eta-2}}\cdots d_{z_1i} + d_{i\,i-1}d_{i-1\,i-2}\cdots d_{j+2\,j+1}d_{j+1\,j}\,.$$

A number of coefficients R_{ji} calculated by the program COIN for the ^{152}Gd decay scheme are shown in table 1 in ref. [63].

Now let us consider the angular-correlation coefficient in our experimental conditions. It can be written as follows:

$$W(\Theta) = 1 + Q_{22}A_{22}P_2(\cos(\Theta)) + Q_{44}A_{44}P_4(\cos(\Theta))\,,$$

$$Q_{22} = Q_2(\text{Det } X)Q_2(\text{Det } Y)\,,$$

$$Q_{44} = Q_4(\text{Det } X)Q_4(\text{Det } Y)\,,$$

where Q_{22} and Q_{44} are the attenuation coefficients taking into account the finite size of the detectors. We calculated Q_2 and Q_4 for the X (CANBERRA) and Y (ORTEC) detectors for a number of energies (d = 35 mm) by the method of Krane [64] using the program SAC [65].

Thus, assuming the average values $Q_{22} = 0.4686$ and $Q_{44} = 0.0224$ take the angular-correlation coefficient in the form

$$W(100^\circ) = 1 - 0.2131A_{22} + 0.00596A_{44}\,.$$

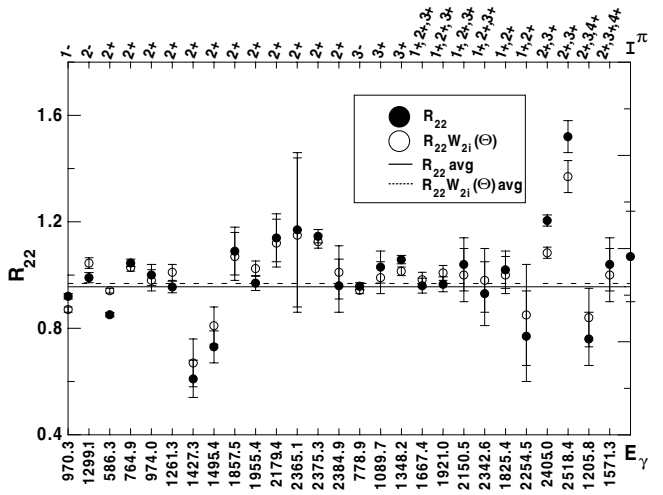

Fig. 3. Branching ratios R_{22} and $R_{22}W_{2i}(\Theta)$ calculated without and with taking into account angular correlations of γ-quanta coupling the first-excited state.

When calculating $W(100^\circ)$ for the transition $I^\pi - (L) \to 2^+ - (2) \to 0^+$ we used the A_{22} and A_{44} from [66], see table 3 in ref. [63]. The $(R_{22})_{\rm exp}$ values were calculated without taking into account the angular correlation between gamma-rays with energies E_{i2} and E_{21} ($W_{i2,21}(100^\circ) = 1$). Then the average $\overline{(R_{22})}_{\rm exp} = 0.956(20)$ with $\chi^2 = 22.7$. After that we corrected them for angular correlation dividing $(R_{22})_{\rm exp}$ by $W_{i2,21}(100^\circ)$, then the average $\overline{[(R_{22})_{\rm exp}/W_{i2,21}(100^\circ)]} = 0.968(15)$ with $\chi^2 = 11.4$. When the multipolarity of the transitions or/and the spin of the levels are uncertain, we choose from the possible set of their values just those giving the ratio $(R_{22})_{\rm exp}/W_{i2,21}(100^\circ)$ closer to 0.97. The values of $(R_{22})_{\rm exp}$ and $(R_{22})_{\rm exp}/W(100^\circ)$ for the transitions $I^\pi(L) \to 2^+(2) \to 0^+$ are shown in fig. 3. I^π is the spin and parity of the initial level. These R_{22} should be the same for each shown transition, therefore in several cases they differ significantly from each other, sometimes by 2σ. This fact could be explained as a result of the cascade transition intensity weakening which has not been taken into account in (1). It also appears if one calculates the ratio of the detector efficiencies, as shown in fig. 2 in ref. [63]. Although the discrepancy in R_{22} values somewhat decreased, finally good agreement was not reached. Probably, the too low R_{22} in the case of 271 keV and 411 keV can be explained by the dependence of the coincidence efficiency on the γ-quanta energy. Our experimental conditions therefore do not allow fully quantitative estimation of such dependence.

Those γ-quanta close in energy which cannot be resolved in single γ-spectra (due to limited energy resolution of the detectors) can however show up in $\gamma\gamma$-coincidence spectra. When the intensities of the components of double and triple peaks are being determined, an additional uncertainty often arises from an indefinite angular-correlation correction factor of the coincident γ-quanta. The analysis of the transitions that feed the first-excited state in ^{152}Gd gave that factor about $\pm 20\%$ of

their average intensity. It appeared that different single γ-transitions feeding the same level have nearly equal values of the experimental coincidence intensity ratios $\frac{S_{\gamma\gamma}(E_{if},E_{f2})}{S_{\gamma\gamma}(E_{if},E_{21})}$. The mean values of such ratios are shown in table 4 in ref. [63].

We used these ratios to split intensities of the double and triple γ-lines into individual ones, because we are able to estimate experimentally only $S_{\gamma\gamma}(E_{if},E_{f2})_{\rm exp}$, $S_{\gamma\gamma}(E_{i'f'},E_{f'2})_{\rm exp}$ and the sum $\{S_{\gamma\gamma}(E_{if},E_{21})+S_{\gamma\gamma}(E_{i'f'},\ E_{21})\}_{\rm exp}$. Let us introduce this ratio:

$$C(E_{f2},E_{21}) \equiv \left\{\frac{S_{\gamma\gamma}(E_{if},E_{f2})}{S_{\gamma\gamma}(E_{if},E_{21})}\right\}_{\rm avg}. \qquad (3)$$

As (3) was written for the single averaged transitions E_{if}, for a double one we can write

$$A_{\rm exp}(E_{if},E_{f2}) \equiv \left\{\frac{S_{\gamma\gamma}(E_{if},E_{f2})}{S_{\gamma\gamma}(E_{if},E_{21})+S_{\gamma\gamma}(E_{i'f'},E_{21})}\right\}_{\rm exp},$$

$$A_{\rm exp}(E_{i'f'},E_{f'2}) \equiv \left\{\frac{S_{\gamma\gamma}(E_{i'f'},E_{f'2})}{S_{\gamma\gamma}(E_{if},E_{21})+S_{\gamma\gamma}(E_{i'f'},E_{21})}\right\}_{\rm exp}.$$

Thus, the intensities of the components of a doublet E_{if} and $E_{i'f'}$ can be derived from the relations:

$$\frac{A_{\rm exp}(E_{if},E_{f2})}{C(E_{f2},E_{21})} = \frac{I_\gamma(E_{if})}{I_\gamma(E_{if}\approx E_{i'f'})},$$

$$\frac{A_{\rm exp}(E_{i'f'},E_{f'2})}{C(E_{f'2},E_{21})} = \frac{I_\gamma(E_{i'f'})}{I_\gamma(E_{if}\approx E_{i'f'})},$$

where the doublet γ-transition intensity is $I_\gamma(E_{if}\approx E_{i'f'}) = I_\gamma(E_{if})+I_\gamma(E_{i'f'})$. Similarly, we also calculated the components of the triplets.

The coincidence intensity ratio in the case using the whole coincidence matrix (summation of X and Y spectra) can be calculated by the equation

$$\frac{S^{\bar X\bar Y}_{\gamma\gamma}(E_{if},E_{f2})}{S^{\bar X\bar Y}_{\gamma\gamma}(E_{if},E_{21})} = \frac{S^X_\gamma(E_{f2})\left\{\frac{\varepsilon^Y_\gamma(E_{f2})}{\varepsilon^X_\gamma(E_{f2})}+\frac{\varepsilon^Y_\gamma(E_{if})}{\varepsilon^X_\gamma(E_{if})}\right\}}{S^X_\gamma(E_{21})\left\{\frac{\varepsilon^Y_\gamma(E_{21})}{\varepsilon^X_\gamma(E_{21})}+\frac{\varepsilon^Y_\gamma(E_{if})}{\varepsilon^X_\gamma(E_{if})}\right\}} \times\frac{R_{ff}W_\gamma(E_{if},E_{f2})}{R_{f2}W_\gamma(E_{if},E_{21})}.$$

Here we assumed the ratio

$$W_\gamma(E_{if},E_{f2})/W_\gamma(E_{if},E_{21}) \approx W_\gamma(E_{i'f'},E_{f'2})/W_\gamma(E_{i'f'},E_{21}).$$

$A_{22}P_2(\cos 100^\circ)$ differs from $A_{44}P_4(\cos 100^\circ)$ by a factor of 3 or less, but since Q_{44} is approximately 28 times smaller than Q_{22}, one can neglect the term $Q_{44}A_{44}P_4$ $(\cos 100^\circ)$.

Thus, when calculating intensities of the components of the double peaks from the coincidence intensity ratios (as given above), we found that the angular-correlation factor (4) does not depend on the spin and parity of the i-th level and on the multipolarity of the upper γ-transition

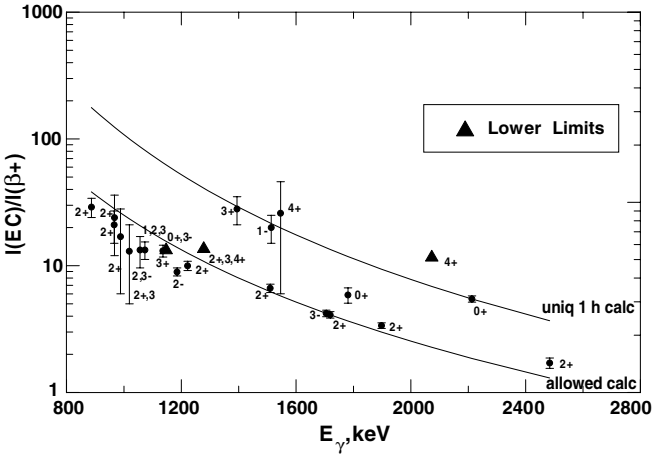

Fig. 4. Experimental (dots) and calculated (curves) ratios of K-electron capture to positron decay intensities for ground and excited states.

(L_{if},L'_{if}):

$$\frac{W(E_{if},E_{f2})-1}{W(E_{if},E_{21})-1} = \frac{A_2(L_{if}L'_{if}I_iI_f)}{A_2(L_{if}L'_{if}I_iI_f)}\cdot\frac{A_2(L_{f2}L'_{f2}2I_f)}{U_2(I_f2)A_2(2202)} = \frac{A_2(L_{f2}L'_{f2}2I_f)}{U_2(I_f2)A_2(2202)} = \frac{W(E_{i'f},E_{f2})-1}{W(E_{i'f},E_{21})-1}, \qquad (4)$$

where $U_2(I_f2)$ is a factor referring to an unobserved transition E_{I_f2}.

Intensities of double and triple γ-lines resolved by the $\gamma\gamma$-coincidences are also given in table 3 below. We found 19 double lines (13 new) and 3 triple ones. We consider the transition of 1598 keV, identified in [6] as a doublet, to be single, since no coincidences of its second component with either γ970 or γ1314 were observed.

Measuring the β^+/EC decay of neutron-deficient nuclei like ^{152}Tb, one can also observe annihilation quanta following positron emission. The intensity of coincidences with such quanta $S^{\bar X,\bar Y}_{511,\gamma}$ has the general form (similar to (1))

$$\frac{S^{\bar X,\bar Y}_{511,\gamma}(511,E_{lk})}{[S^X_\gamma(511)S^Y_\gamma(E_{lk})+S^Y_\gamma(511)S^X_\gamma(E_{lk})]} \times\left[\frac{I_\gamma(511)}{NT}\right]^{-1} = \sum_{i=l}^{m} R_{il}I_\beta(i), \qquad (5)$$

where $I_\beta(i)$ is the intensity of the β-transition to the i-th level, R_{il} is the branching coefficient calculated by (2). The intensity of a transition is expressed by (5), at first for the highest level excited in the decay and consecutively downward to the first (lowest) one. Intensities of the β^+-transitions (or their upper limits) were found (see table 1) for level energies up to 2300 keV.

In the general case we do not know the absolute intensity of annihilation quanta, but we can determine $\frac{I(\rm EC)}{I(\beta)}$ in relative units first. To deduce this normalizing coefficient, we assume that this experimental ratio for allowed

Table 1. Relative intensities of β^+-transitions to the levels up to 2300 keV.

$i_{\rm lev}$	I^π	$E_{\rm lev}$	$I_\beta(i)$	$i_{\rm lev}$	I^π	$E_{\rm lev}$	$I_\beta(i)$
2	2^+	344.280	118901(11200)	24	2^+	1771.557	394(110)
3	0^+	615.373	19026(1084)	25	2^+	1785.24	285(39)
4	4^+	755.395	−94(253)	26		1807.53	< 62
5	2^+	930.550	35900(1967)	27		1808.95	427(126)
6	0^+	1047.774	3623(500)	28	2^+	1839.70	542(144)
7	2^+	1109.193	10865(560)	29	2^+	1861.897	< 370
8	3^-	1123.183	6047(356)	30	2^+	1862.06	697(100)
9		1227.37	< 314	31		1915.19	< 73
10		1274.2	< 114	32		1915.69	< 66
11	4^+	1282.267	134(100)	33	2^+	1941.157	2062(400)
12	1^-	1314.635	467(96)	34		1975.67	< 77
13	2^+	1318.349	7639(969)	35		2011.65	< 192
14	3^+	1434.017	408(102)	36		2120.96	< 16
15	2^+	1470.61	842(69)	37		2133.39	< 104
16		1533.91	< 183	38		2169.58	< 17
17		1550.15	< 378	39	2^+	2201.73	< 32
18	2^+	1605.584	4078(680)	40	2^+	2246.772	< 453
19	2^-	1643.427	3168(231)	41		2258.14	< 9
20		1680.76	< 187	42		2264.83	< 3
21	3^+	1692.42	776(79)	43		2265.28	< 4
22		1734.44	< 20	44		2267.71	< 5
23		1755.73	441(71)	45	2^+	2299.636	< 56

transitions is equal to the theoretical one (within approximately 10% errors, see [67], [68] and fig. 27 therein). We used the allowed transition to the 3^- final state for such normalization. In accordance with table XXI from [68], for some nuclei the ratio analyzed in the case of allowed transitions almost does not differ from that of 1st-forbidden non-unique ones (within the error limits), while for others it may differ by up to 30%. Experimental ratios of electron capture to positron emission intensities are compared to the theoretical ratios for allowed unhindered (au) and unique first-forbidden (1^*h) β-transitions, see fig. 4.

For each 91 resulting coincidence spectra $S_{\gamma\gamma}^{\bar{X},\bar{Y}}$ and $\sigma(S_{\gamma\gamma}^{\bar{X},\bar{Y}})$ were found and $(R_{ji})_{\rm exp}$ calculated by (1) with $W(\Theta) = 1$.

At the first stage of analysis we thoroughly checked the results of the $\gamma\gamma$-coincidence analysis performed in [6]. The direct transitions which feed the ^{152}Gd ground state were unambiguously confirmed by the $\gamma\gamma$-coincidences with the upper transition gated as shown in table 2.

Coincidences of the transitions chosen as gates with the lower transitions proved the placements of the following transitions: 271.09, 411.1165, 526.85, 543.58, 586.27, 622.79, 675.01, 703.39, 764.89, 778.9045, 794.73, 909.15, 970.32, 974.05, 990.19, 1052.15, 1137.56, 1159.82, 1190.44, 1209.03, 1299.140, 1325.86, 1348.15, 1586.22, 1631.42, 1739.46, 1757.42, 1841.15, 1857.48, 2033.89 and 2251.41 keV.

Part of the $\gamma\gamma$-coincidence results is given in table 9 in ref. [63]. We determined the experimental ratio $(R_{ji}/R_{22})_{\rm exp}$ (see eq. (1)) for transitions which coincide with the most intense transitions de-exciting the low-energy levels. The experimental ratios were compared with the calculated ones and the qualifying transitions were then placed in the decay scheme. The decay scheme in a tabular form is shown in table 3.

Table 2. Direct transitions to the ^{152}Gd ground state confirmed by $\gamma\gamma$-coincidences.

Direct transition (keV)	Gate (keV)
1318.24	622.79
930.58	675.01, 909.15, 2033.89
1109.20	1190.44
1314.66	1209.03
344.2785	2405.00, 2518.42

Obviously, energies and multipolarities of the transitions placed between the levels with known energies, spins and parities follow the energy balance, the balance of total transition intensities and the momentum and parity conservation law. Zolnowski *et al.* [6] introduced 41 levels on the basis of the $\gamma\gamma$-coincidences and 25 more levels were introduced tentatively on the basis of energy balance. Our measurements of $\gamma\gamma$-coincidences confirmed 40 levels, and only the 3411.5 keV level was not confirmed. Out of all the tentatively introduced levels [6] four levels at 1771.557, 1975.67, 2264.83 and 2932.66 keV agree with our $\gamma\gamma$-coincidence results. Based on the $\gamma\gamma$-coincidences, we introduced 46 new levels. Using the conservation laws we found unique or possible spins and parities for all levels. Placement of 58 transitions on the basis of $\gamma\gamma$-coincidences and 53 transitions on the basis of mere energy balance [6] was confirmed by our $\gamma\gamma$-coincidences. In addition, we placed 131 transitions on the basis of coincidences for the first time. Thus, 242 gamma-transitions have been unambiguously (on the basis of $\gamma\gamma$-coincidences) placed in the ^{152}Tb $\rightarrow$ ^{152}Gd decay scheme, see table 3.

Table 3. Decay scheme of ^{152}Gd.

No.	E_i (keV)	I^π	I_β	log ft	E_γ (keV)	Type	$I_\gamma \pm \Delta I_\gamma$	$\alpha_K(\Delta\alpha_K)$	XL	E_f (keV)
1	0	0^+	29.9(19)	7.53						
2	344.280(2)	2^+	13.3(17)	7.75	344.279	c	100.0 ± 2.50	3.13(30)E-2	$E2$	0
3	615.373(18)	0^+	6.8(3)	7.95	615.6	b,p	0.03 ± 0.00	> 437(25)	$E0$	0
					271.09	c,p	99.97 ± 2.20	6.0(9)E-2	$E2$	344.28
4	755.395(2)	4^+	0.39(9)	9.29	411.1165	a,c,p	100.0 ± 2.47	1.92(23)E-2	$E2$	344.28
5	930.550(13)	2^+	7.9(3)	7.8	930.58	c,p	12.72 ± 0.44	4.0(8)E-3	$E2$,$M1$	0
					586.27	c,p	80.04 ± 1.65	2.02(21)E-2	$M1(E0)$	344.28
					315.16	c,p	7.04 ± 0.15	5.2(18)E-2	$E2(M1)$	615.373
					175.14	n,c,p	0.21 ± 0.02	4.3(9)E-1	$M1$	755.395
6	1047.774(27)	0^+	1.39(9)	8.53	1047.9	b,p	0.53 ± 0.00	> 2.06(20)	$E0$	0
					703.494	d,c,p	96.17 ± 2.84	d	$E2$	344.28
					432.5	b,p	0.12 ± 0.00	> 237(24)	$E0$	615.373
					117.25	p	3.19 ± 0.09	6.4(10)E-1	$E2$	930.55
7	1109.193(15)	2^+	2.78(12)	8.21	1109.2	c,p	46.54 ± 1.04	2.3(4)E-3	$E2$,$M1$	0
					764.89	c,p	50.14 ± 1.16	5.7(13)E-3	$E2$,$M1$	344.28
					493.81	c,p	2.59 ± 0.07	d		615.373
					353.78	n,c,p	0.52 ± 0.02			755.395
					178.58	n,p	0.22 ± 0.02	1.8(11)	$E2$,$M1$	930.55
8	1123.183(4)	3^-	1.66(14)	8.45	778.9045	a,c,p	94.07 ± 1.94	1.48(24)E-3	$E1$	344.28
					367.8	c,p	5.93 ± 0.15	1.2(4)E-2	$E1$	755.395
9	1227.37(8)	6^+	< 0.005	> 10.9	471.98	c,p	100.0 ± 4.14			755.395
10	1274.25(8)	2^+	< 0.009	> 11.4	658.83	c,p	100.0 ± 6.70			615.373
11	1282.267(28)	4^+	0.232(15)	9.22	526.85	c,p	52.10 ± 1.13	8.2(9)E-2	$E0 + M1$	755.395
					351.73	c,p	46.06 ± 1.13	3.0(10)E-2	$E2$	930.55
					159.16	n,p	1.85 ± 0.20			1123.183
12	1314.635(20)	1^-	0.69(5)	8.81	1314.635	d,c,p	58.58 ± 2.20	t	$(E1)$	0
					970.32	c,p	37.45 ± 0.79	1.4(5)E-3	$E1$	344.28
					699.25	c,p	3.97 ± 0.28	d		615.373
13	1318.349(17)	2^+	2.89((13)	8.12	1318.24	c,p	5.35 ± 0.22	3.1(6)E-3	$M1$	0
					974.05	c,p	60.11 ± 1.27	5.0(6)E-3	$M1$	344.28
					702.976	d,c,p	17.07 ± 0.64	d	$E2$	615.373
					562.98	c,p	1.34 ± 0.04			755.395
					387.8	c,p	7.46 ± 0.25	0.42(11)	$E0 + M1$	930.55
					209.14	c,p	0.72 ± 0.03	3.0(5)E-1	$M1(E0)$	1109.193
					195.17	c,p	7.95 ± 0.18	d	$E1$	1123.183
14	1434.017(8)	3^+	0.75(4)	8.66	1089.737	a,c,p	73.10 ± 1.50	2.7(5)E-3	$E2$,$M1$	344.28
					678.61	c,p	18.24 ± 0.41	7.4(29)E-3	$E2(M1)$	755.395
					503.43	c,p	5.25 ± 0.14			930.55
					324.9	n,c,p	3.42 ± 0.15			1109.193
15	1470.61(5)	2^+	< 0.019	> 8.66	855.237	t,c,p	31.20 ± 6.07	d		615.373
					715.19	c,p	68.80 ± 1.73			755.395
16	1533.91(11)		< 0.003	> 11.7	603.18	n,c,p	100.0 ± 6.86			930.55
17	1550.15(4)	$2^+, 3, 4^+$	0.287(11)	9.04	1205.83	c,p	33.75 ± 1.34	2.5(11)E-3	$E1(E2)$	344.28
					794.73	c,p	52.54 ± 1.34			755.395
					441.02	c,p	13.71 ± 0.36			1109.193
18	1605.584(18)	2^+	2.30(8)	8.12	1605.584	d,c,p	8.31 ± 1.19	d	$E1(E2)$	0
					1261.32	c,p	33.72 ± 0.71	2.2(4)E-3	$M1$	344.28
					990.19	c,p	26.69 ± 0.55	1.9(5)E-3	$E2$	615.373
					850.49	n,c,p	1.12 ± 0.09			755.395
					675.01	c,p	19.83 ± 0.40	6.0(15)E-3	$E2$	930.55
					557.81	d,c,p	2.71 ± 0.26			1047.774
					496.37	c,p	5.46 ± 0.12	d	$E0 + M1$	1109.193
					482.34	c,p	2.17 ± 0.05			1123.183
19	1643.427(13)	2^-	1.85(7)	8.19	1299.14	a,c,p	90.12 ± 1.94	5.9(11)E-4	$E1$	344.28
					712.82	c,p	4.91 ± 0.17			930.55
					534.21	c,p	2.29 ± 0.06			1109.193
					520.3	c,p	2.69 ± 0.11			1123.183

Table 3. Continued.

No.	E_i (keV)	I^π	I_β	log ft	E_γ (keV)	Type	$I_\gamma \pm \Delta I_\gamma$	$\alpha_K(\Delta\alpha_K)$	XL	E_f (keV)
20	1680.76(5)		0.167(6)	9.18	1336.54	c,p	74.61 ± 1.52			344.28
					750.06	n,c,p	7.50 ± 0.76			930.55
					366.15	n,c,p	17.89 ± 0.99			1314.635
21	1692.42(3)	3^+	0.67(3)	8.59	1348.15	c,p	83.99 ± 1.69	1.20(22)E-3	$E2$	344.28
					937.04	c,p	16.01 ± 0.63			755.395
22	1734.44(16)		0.026(2)	10	979.04	n,p	100.0 ± 5.77			755.395
23	1755.76(7)	$1^-, 2^-, 3$	0.38(3)	8.91	1411.48	d,c,p	100.0 ± 5.88	d	$E1$	344.28
24	1771.557(26)	2^+	0.343(12)	8.88	1427.32	c,p	30.66 ± 0.74			344.28
					841.1	c,p	13.38 ± 0.74			930.55
					723.67	n,p	5.98 ± 0.24			1047.774
					648.31	c,p	30.85 ± 0.74			1123.183
					489.59	n,c,p	7.06 ± 0.56			1282.267
					456.92	c,p	12.06 ± 0.50			1314.635
25	1785.24(11)	2^+	0.043(6)	9.78	854.69	t,c,p	61.56 ± 12.01	d	$E0+M1$	930.55
					662.02	n,p	38.44 ± 4.20			1123.183
26	1807.53(5)		0.105(4)	9.88	1052.15	c,p	100.0 ± 2.16			755.395
27	1808.95(8)		0.062(4)	9.6	878.13	n,c,p	29.23 ± 2.31			930.55
					490.66	c,p	70.77 ± 2.31			1318.349
28	1839.70(4)	2^+	0.267(17)	8.98	1495.44	c,p	33.33 ± 1.23	4.7(9)E-3	$E0+M1$	344.28
					1084.305	n,d,c,p	14.31 ± 3.27			755.395
					909.15	c,p	39.88 ± 1.23			930.55
					557.433	d,c,p	12.47 ± 2.45		$M1(E2)$	1282.267
29	1861.897(28)	2^+	0.99(3)	8.38	1861.94	c,p	46.53 ± 0.97	8.5(24)E-4	$E2$,$M1$	0
					814.123	n,d,c,p	2.46 ± 0.45			1047.774
					752.59	n,c,p	3.23 ± 0.26			1109.193
					738.69	c,p	21.72 ± 0.58			1123.183
					579.63	n,c,p	3.04 ± 0.16			1282.267
					543.58	c,p	19.58 ± 0.45	d	$(E0M1)$	1318.349
					427.85	n,c,p	2.04 ± 0.14			1434.017
					218.42	n,p	1.41 ± 0.07			1643.427
30	1862.06(4)	2^+	0.96(5)	8.39	1517.78	t,c,p	52.72 ± 3.95	d	$M1$	344.28
					1106.59	c,p	39.94 ± 1.19			755.395
					547.47	c,p	7.34 ± 0.19	d		1314.635
31	1915.19(4)	$4^+, 5, 6^+$	0.179(12)	9.1	1159.82	c,p	96.48 ± 2.35			755.395
					687.62	n,p	3.52 ± 0.94			1227.374
32	1915.69(4)	$2^+, 3, 4^+$	0.156(7)	9.16	1571.25	c,p	76.24 ± 1.53			344.28
					792.56	n,c,p	9.64 ± 0.61			1123.183
					633.6	p	8.97 ± 0.34			1282.267
					597.57	n,p	5.14 ± 0.34			1318.349
33	1941.157(18)	2^+	4.25(14)	7.71	1941.23	c,p	16.30 ± 0.34	4.7(11)E-4	$(E2)$	0
					1596.877	d,c,p	7.03 ± 0.37	1.01(23)E-3	$E1$,$E2$	344.28
					1325.86	c,p	18.23 ± 0.38	1.6(4)E-3	$E2(M1)$	615.373
					1185.73	c,p	4.96 ± 0.12	1.2(4)E-3	$E2(E1)$	755.395
					1010.6	c,p	9.30 ± 0.19	5.7(14)E-3	$M1$	930.55
					893.34	c,p	14.85 ± 0.31	7.3(11)E-3	$(M1)$	1047.774
					831.94	c,p	2.63 ± 0.07			1109.193
					817.974	d,c,p	2.21 ± 0.37			1123.183
					622.79	c,p	21.33 ± 0.44	1.09(17)E-2	$E2$,$M1$	1318.349
					390.82	n,c,p	0.17 ± 0.03			1550.15
					335.56	n,c,p	1.37 ± 0.04			1605.584
					298.06	n,p	0.16 ± 0.02			1643.427
					248.75	c,p	1.46 ± 0.18			1692.417
34	1975.67(5)	$1^+, 2^+$	0.174(8)	9.04	1975.65	c,p	43.24 ± 0.95			0
					1631.39	d,c,p	39.84 ± 2.92	1.07(21)E-3	$E2$,$M1$	344.28
					1360.43	c,p	16.92 ± 0.77	d		615.373
35	2011.65(4)	$1^+, 2^+, 3$	0.82(3)	8.4	1667.38	c,p	76.46 ± 1.77	1.30(24)E-3	$M1$	344.28
					902.46	c,p	16.64 ± 0.44			1109.193
					697.2	n,c,p	1.77 ± 0.59	d		1314.635
					693.13	c,p	3.10 ± 0.21			1318.349
					577.57	n,c,p	2.03 ± 0.10			1434.017

Table 3. Continued.

No.	E_i (keV)	I^π	I_β	log ft	E_γ (keV)	Type	$I_\gamma \pm \Delta I_\gamma$	$\alpha_K(\Delta\alpha_K)$	XL	E_f (keV)
36	2120.96(10)	$2^+, 3, 4^+$	0.091(5)	9.24	1776.3	n,p	12.78 ± 1.67			344.28
					1365.69	c,p	75.56 ± 1.67			755.395
					839.6	n,c,p	11.67 ± 2.22			1282.267
37	2133.39(10)	$1^+, 2^+$	0.530(24)	8.53	1789.11	d,c,p	88.0 ± 2.33	d	$E2$,$M1$	344.28
					1518.017	t,c,p	5.83 ± 1.17	d		615.373
					1202.84	d,c,p	5.01 ± 1.40			930.55
					818.755	d,c,p	1.17 ± 0.47			1314.635
38	2169.58(6)	$1, 2^+$	0.144(8)	9.05	1825.37	c,p	83.42 ± 1.75			344.28
					1554.04	n,p	7.47 ± 0.67			615.373
					854.945	t,c,p	9.11 ± 2.45	d		1314.635
39	2201.73(5)	2^+	0.292(13)	8.76	2201.65	n,p	4.17 ± 0.42			0
					1857.48	c,p	57.04 ± 1.26	7.6(28)E-4	$E2$,$M1$	344.28
					1446.335	d,c,p	27.47 ± 2.73	1.3(3)E-3	$E2(M1)$	755.395
					1092.26	n,c,p	11.32 ± 0.63			1109.193
40	2246.772(23)	2^+	3.74(13)	7.63	1902.492	d,c,p	45.09 ± 1.02	9.2(17)E-2	$M1$	344.28
					1631.399	d,c,p	4.27 ± 0.25	1.07(21)E-3	$E2$,$M1$	615.373
					1491.62	n,c,p	0.45 ± 0.03			755.395
					1316.32	c,p	5.25 ± 0.41	t		930.55
					1137.56	c,p	22.87 ± 0.49	3.0(6)E-3	$M1$	1109.193
					932.09	c,p	5.17 ± 0.19			1314.635
					928.43	c,p	9.63 ± 0.20	3.7(18)E-3	$E2$,$M1$	1318.349
					812.8	c,p	5.32 ± 0.14			1434.017
					641.2	c,p	1.58 ± 0.04			1605.584
					407.12	n,c,p	0.37 ± 0.05			1839.704
41	2258.14(6)	$2^+, 3, 4^+$	0.091(6)	9.23	1502.62	n,c,p	16.67 ± 0.56			755.395
					1148.99	c,p	46.53 ± 2.08			1109.193
					939.84	n,c,p	36.81 ± 1.25			1318.349
42	2264.83(7)	$1^-, 2, 3^-$	0.013(5)	10.1	1141.68	n,c,p	61.60 ± 2.83			1123.183
					950.34	n,p	26.74 ± 1.18			1314.635
					947.08	n,p	11.66 ± 2.12			1318.349
43	2265.28(9)	$1^+, 2^+, 3$	0.42(5)	8.57	1921	c,p	100.0 ± 2.12	9.2(21)E-4	$M1(E2)$	344.28
44	2267.71(8)		0.067(3)	9.36	1040.6	n	9.46 ± 1.99			1227.374
					953.07	d,c,p	90.54 ± 2.27	5.6(8)E-3	$M1$	1314.635
45	2299.636(26)	2^+	0.99(3)	8.17	1955.36	c,p	34.20 ± 0.75	3.1(9)E-4	$E1(E2)$	344.28
					1369.04	c,p	12.48 ± 0.31	2.6(7)E-3	$M1$	930.55
					1190.44	c,p	37.70 ± 0.75			1109.193
					1176.53	n,p	2.70 ± 0.11			1123.183
					984.9	c,p	5.80 ± 0.31			1314.635
					865.62	n,c,p	3.76 ± 0.15			1434.017
					656.42	p	3.35 ± 0.15			1643.427
46	2325.82(9)		< 0.003	> 10.7	1202.64	d,c,p	100.0 ± 21.74			1123.183
47	2330.70(8)	$2^+, 3, 4^+$	0.064(3)	9.35	1986.8	n,p	7.39 ± 1.48			344.28
					1575.3	c,p	92.61 ± 2.46			755.395
48	2386.95(11)	$1^-, 2, 3^-$	0.159(8)	8.92	2042.67	t,c,p	43.82 ± 3.19			344.28
					1263.84	n,c,p	43.82 ± 1.59			1123.183
					1072.16	n,c,p	12.35 ± 1.59			1314.635
49	2401.49(6)	$1^+, 2, 3^-$	0.201(11)	8.81	1087.12	c,p	65.38 ± 2.53			1314.635
					1083.141	n,d,c,p	16.42 ± 3.79			1318.349
					708.98	c,p	18.19 ± 0.66			1692.417
50	2437.44(6)	$1^+, 2^+$	0.42(4)	8.47	2437.11	n,p	1.99 ± 0.15			0
					2093.16	d,c,p	31.86 ± 2.72	1.25(24)E-3	$(M1)$	344.28
					1506.9	c,p	11.78 ± 0.44	2.7(5)E-3	$M1$	930.55
					1314.257	d,c,p	54.36 ± 7.55	t	$E1$	1123.183
51	2447.82(12)		< 0.018	9.83	2103.54	d,c,p	100.0 ± 21.28	6.0(14)E-4	$E2(M1)$	344.28
52	2495.17(5)	$1^+, 2^+, 3$	0.272(10)	8.63	2150.85	c,p	81.99 ± 1.63	6.6(12)E-4	$M1(E2)$	344.28
					1372.04	c,p	18.01 ± 0.54	1.9(5)E-3		1123.183

Table 3. Continued.

No.	E_i (keV)	I^π	I_β	log ft	E_γ (keV)	Type	$I_\gamma \pm \Delta I_\gamma$	$\alpha_K(\Delta\alpha_K)$	XL	E_f (keV)
53	2513.9(3)	$1^+, 2^+$	0.045(12)	9.4	2513.9	n,p	9.99 ± 2.53			0
					2169.16	d,c,p	90.01 ± 25.32	5.6(13)E-4	$E2$,$M1$	344.28
54	2523.80(4)	2^+	0.676(24)	8.21	2523.92	p	12.27 ± 0.28	5.1(10)E-4	$M1(E2)$	0
					2179.42	c,p	8.71 ± 0.23	d	$M1$	344.28
					1593.37	n,c,p	13.58 ± 0.37			930.55
					1400.617	d,c,p	14.42 ± 1.22			1123.183
					1209.03	c,p	42.42 ± 0.94	4.9(21)E-4	$E1$	1314.635
					880.29	n,p	6.08 ± 0.20			1643.427
					684.12	n,p	2.53 ± 0.28			1839.704
55	2529.39(3)		0.183(7)	8.2	2185.24	c,p	32.75 ± 0.64	5.8(17)E-4	$E2$,$M1$	344.28
					1598.9	c,p	31.66 ± 0.73			930.55
					1406.16	c,p	14.64 ± 0.37	1.2(5)E-3	$E2(E1)$	1123.183
					1247.07	c,p	19.12 ± 0.55			1282.267
					722	n,c,p	1.83 ± 0.13			1807.533
56	2540.45(6)	$2^+, 3^+$	0.183(7)	8.77	2196.2	c,p	50.95 ± 1.04	1.01(29)E-3	$M1$	344.28
					1785.15	n,c,p	26.69 ± 1.39			755.395
					1417.18	n,c,p	10.85 ± 0.55			1123.183
					1221.95	n,c,p	11.51 ± 0.76			1318.349
57	2544.00(7)		0.107(4)	9	1613.53	n,p	48.87 ± 1.66			930.55
					1420.76	c,p	51.13 ± 1.42			1123.183
58	2551.12(6)		0.139(5)	8.88	1441.91	c,p	83.14 ± 2.28			1109.193
					1117.15	n,c,p	16.86 ± 0.64			1434.017
59	2557.84(4)	2^+	0.172(6)	8.79	2557.91	p	14.50 ± 0.45			0
					2211.7		0.0	$> 3(1)E$-2	$(E0 + M1)$	344.28
					1802.67	c,p	38.17 ± 1.01			755.395
					1434.54	n,c,p	16.81 ± 0.82			1123.183
					914.35	p,c	30.53 ± 0.89			1643.427
60	2598.78(5)	1^+,2^+	0.289(10)	8.64	2254.54	c,p	32.18 ± 0.64	d	$E2$,$M1$	344.28
					1983.41	c,p	24.50 ± 0.58			615.373
					1489.6	c,p	22.09 ± 0.64	2.2(8)E-3	$M1(E2)$	1109.193
					993.14	n,c,p	21.24 ± 0.86			1605.584
61	2604.33(5)	$1^-, 2, 3^-$	0.158(6)	8.79	2260.05	c,p	41.77 ± 1.00			344.28
					1481.18	p,c	39.25 ± 2.00			1123.183
					1289.64	c,p	18.98 ± 0.60			1314.635
62	2641.56(7)		0.132(9)	8.85	1711.02	n,c,p	16.11 ± 0.53			930.55
					1518.377	t,c,p	83.89 ± 6.23	d	$E2$,$M1$	1123.183
63	2667.54(6)	1^-	0.131(6)	8.83	1737.03	n,c,p	31.78 ± 0.82			930.55
					1544.29	c,p	45.90 ± 1.12			1123.183
					1352.98	n,c,p	22.32 ± 2.43	1.9(4)E-2	$E0 + M1$	1314.635
64	2686.85(10)	$1^+, 2^+, 3$	0.129(10)	8.83	2342.57	c,p	100.0 ± 1.97	1.32(26)E-3	$M1(E0)$	344.28
65	2709.42(3)	2^+	1.64(6)	7.69	2709.47	p	10.55 ± 0.23	2.7(8)E-4	$E1(E2)$	0
					2365.13	c,p	21.94 ± 0.54	1.2(3)E-3	$E0 + M1$	344.28
					2094.047	d,c,p	4.70 ± 0.42			615.373
					1778.78	c,p	6.35 ± 0.19	1.6(4)E-3	$M1$	930.55
					1586.22	c,p	55.81 ± 1.15	4.5(9)E-4	$E1$	1123.183
					1066.23	n,p	0.66 ± 0.05			1643.427
66	2719.67(4)	2^+	1.38(5)	7.77	2719.61	p	18.38 ± 0.41	3.7(11)E-4	$E1$,$E2$	0
					2375.34	c,p	56.15 ± 1.19	7.9(18)E-4	$M1$	344.28
					2104.297	d,c,p	2.48 ± 0.55		$E2(M1)$	615.373
					1789.12	d,c,p	6.60 ± 0.50	d	$E2$,$M1$	930.55
					1596.487	d,c,p	11.14 ± 0.83	t	$E1$,$E2$	1123.183
					1401.321	d,c,p	4.13 ± 0.37			1318.349
					1027.16	n,c,p	0.77 ± 0.09			1692.417
					454.82	n,p	0.36 ± 0.08			2264.833

Table 3. Continued.

No.	E_i (keV)	I^π	I_β	log ft	E_γ (keV)	Type	$I_\gamma \pm \Delta I_\gamma$	$\alpha_K(\Delta\alpha_K)$	XL	E_f (keV)
67	2729.165(29)	2^+	1.02(4)	7.9	2729.25	n	1.66 ± 0.06			0
					2384.94	c,p	9.21 ± 0.19	d	$M1(E0)$	344.28
					2113.7	c,p	8.64 ± 0.19	7.0(17)E-4	$M1(E2)$	615.373
					1798.45	c,p	10.03 ± 0.38	9.2(4)E-4	$E2$,$M1$	930.55
					1681.53	c,p	4.17 ± 0.11			1047.774
					1605.982	d,c,p	14.92 ± 1.91	d	$E1(E2)$	1123.183
					1410.816	c,p	20.96 ± 1.27	d	$E2$,$M1$	1318.349
					1258.45	n,p	4.76 ± 0.18			1470.612
					1085.68	t,c,p	13.65 ± 0.44			1643.427
					1036.74	c,p	10.92 ± 0.25			1692.417
					813.475	n,d,c,p	1.08 ± 0.51			1915.191
68	2734.04(7)	1^+	0.145(5)	8.74	2734.06	p	61.90 ± 1.31	2.5(5)E-4	$E1(E2)$	0
					2118.66	c,p	38.10 ± 1.00	1.0(4)E-3	$M1$	615.373
69	2744.05(11)	1^-	0.084(3)	8.97	2744.1	p	91.86 ± 1.96	1.2(5)E-4	$E1$	0
					1634	n,c,p	8.14 ± 1.89			1109.193
70	2749.20(3)	$2^+, 3^+$	1.58(6)	7.69	2405	c,p	82.62 ± 1.60	3.2(9)E-4	$E1(E2)$	344.28
					1993.87	c,p	5.75 ± 0.12			755.395
					1640.08	c,p	2.73 ± 0.09	2.1(9)E-3	$M1$	1109.193
					1475.04	n,p	0.60 ± 0.20			1274.256
					1430.76	c,p	5.91 ± 0.24			1318.349
					1215.2	n,p	0.66 ± 0.07			1533.918
					1056.79	n,c,p	1.42 ± 0.05			1692.417
					301.82	n,p	0.31 ± 0.09			2448.009
71	2772.36(6)	2^+	0.287(12)	8.42	2772.44	n,p	1.77 ± 0.11			0
					1841.81	d,c,p	9.08 ± 1.11	d	$E2$,$M1$	930.55
					1663.67	c,p	14.83 ± 0.89	7.3(24)E-3	$E0 + M1$	1109.193
					1454.08	n,c,p	7.84 ± 0.44			1318.349
					1338.5	n,p	4.27 ± 0.58			1434.017
					1128.65	n	9.52 ± 1.11			1643.427
					1016.6	c,p	24.80 ± 0.66			1755.73
					857.33	c,p	27.89 ± 1.99	d	$(E0M1)$	1915.191
72	2862.64(5)		0.231(8)	8.42	2518.42	c,p	49.04 ± 1.10	5.0(9)E-4	$M1(E2)$	344.28
					1739.46	c,p	33.26 ± 0.74	1.35(30)E-3	$M1(?)$	1123.183
					1547.95	n,c,p	17.70 ± 0.49			1314.635
73	2869.76(10)	$1, 2^+$	0.064(10)	9	2525.43		0.0			344.28
					2254.44	c,p	100.0 ± 2.00	d		615.379
74	2880.652(21)	1^+,2^+	1.82(6)	7.53	2536.3	c,p	13.75 ± 0.38	6.4(12)E-4	$M1$	344.28
					2265.33	c,p	4.59 ± 0.10			615.373
					1771.43	c,p	18.03 ± 0.38	1.41(27)E-3	$M1$	1109.193
					1757.42	c,p	35.36 ± 0.80	6.3(13)E-4	$(E1)$	1123.183
					1565.97	c,p	5.55 ± 0.01			1314.635
					1562.45	c,p	4.49 ± 0.10	2.3(10)E-3	$M1$	1318.349
					1446.635	d,c,p	8.91 ± 0.90	d	$E2(M1)$	1434.017
					1275.04	c,p	5.39 ± 0.14			1605.584
					1188.37	n,c,p	1.96 ± 0.08			1692.417
					868.94	n,p	1.44 ± 0.05			2011.65
					747.29	n,c,p	0.55 ± 0.04			2133.395
75	2914.15(7)	2^+	0.250(9)	8.4	2914.42	p	3.06 ± 0.15	9(4)E-4	$(M1)$	0
					2569.85	p	63.95 ± 1.52	3.0(6)E-4	$(E1E2)$	344.28
					2158.72	c,p	27.81 ± 0.76	5.4(18)E-4	$E2(M1)$	755.395
					998.37	n,p	5.18 ± 0.28			1915.687
76	2920.08(14)		0.103(5)	8.75	2575.82	p	27.45 ± 1.17			344.28
					1811.33	n,p	15.38 ± 1.85			1109.193
					1796.83	n,c,p	51.08 ± 3.08			1123.183
					1004.2	n,p	6.09 ± 0.92			1915.687

Table 3. Continued.

No.	E_i (keV)	I^π	I_β	log ft	E_γ (keV)	Type	$I_\gamma \pm \Delta I_\gamma$	$\alpha_K(\Delta\alpha_K)$	XL	E_f (keV)
77	2927.85(5)	$2^+, 3^+$	0.264(10)	8.33	2583	p	11.26 ± 1.92			344.28
					2172.45	d,c,p	11.83 ± 0.41			755.395
					1818.56	c,p	22.18 ± 0.67	1.6(6)E-3	$M1$	1109.193
					1457.25	n,p	6.95 ± 0.53			1470.612
					1284.42	c,p	30.42 ± 0.72			1643.427
					1235.57	c,p	17.37 ± 0.60			1692.417
78	2928.68(24)		0.071(6)	8.9	2584.89	p	77.82 ± 7.16			344.28
					1610.11	n,p	22.18 ± 1.88			1318.349
79	2932.66(6)	2^+	0.448(16)	8.1	2588.36	p	80.62 ± 1.69	6.2(11)E-4	($M1$)	344.28
					2317.61	n,c,p	1.45 ± 0.14			615.373
					1809.53	c,p	17.93 ± 0.56			1123.183
80	2964.33(4)	$2^-, 3^-$	0.334(13)	8.21	2033.89	c,p	40.93 ± 0.95	3.6(9)E-4	$E1$	930.55
					1841.147	d,c,p	15.54 ± 1.90	d	$E2$,$M1$	1123.183
					1645.92	c,p	19.90 ± 0.49			1318.349
					1530.07	n,p	2.94 ± 0.25			1434.017
					1414.4	n,c,p	11.20 ± 0.40			1550.15
					1155.48	n,p	6.25 ± 0.76			1808.95
					638.35	n,p	3.24 ± 0.42			2325.928
81	2981.38(9)	$2^+, 3, 4^+$	0.054(2)	8.97	2636.93	p	49.48 ± 1.16			344.28
					2226.01	n,c,p	31.55 ± 2.10			755.395
					860.84	n,p	18.98 ± 1.86			2121.061
82	2989.02(9)		0.039(5)	9.1	2644.74	n,p	44.07 ± 2.76			344.28
					2058.47	n,c,p	24.07 ± 2.11			930.55
					1714.65	n,p	10.73 ± 1.46			1274.256
					1047.9	b,p	21.14 ±	> 2.06(20)		1941.157
83	2999.52(4)	$1^+, 2^+$	0.233(8)	8.32	2999.69	p	13.57 ± 0.22			0
					2655.29	p	23.72 ± 0.68	4.1(12)E-4	$E2$,$M1$	344.28
					2069	c,p	39.45 ± 0.82	7.5(17)E-4	$M1$($E2$)	930.55
					1393.86	n,c,p	19.75 ± 0.52			1605.584
					829.57	n	3.51 ± 0.92			2169.583
84	3006.71(4)	2^+	0.365(13)	8.17	3006.63	n,p	2.05 ± 0.07			0
					2662.55	p	46.64 ± 0.87	2.8(13)E-4	$E1$,$E2$	344.28
					2251.41	c,p	21.86 ± 0.49	d		755.395
					2076.21	c,p	10.28 ± 0.40	d	$E2$,$M1$	930.55
					1732.42	n,p	3.16 ± 0.28			1274.256
					1363.39	n,p	7.13 ± 0.43	d		1643.427
					1167	n,p	3.29 ± 0.69			1839.704
					837.08	n,p	5.60 ± 0.29			2169.583
85	3009.16(6)	$2^-, 3^-$	0.120(5)	8.6	2665.18	n	36.07 ± 0.94			344.28
					2078.63	c,p	17.58 ± 0.81	d		930.55
					1886.08	c,p	15.52 ± 1.01	3.6(11)E-3	$M1$($E0$)	1123.183
					1694.6	n,p	8.91 ± 0.40			1314.635
					1690.68	n,p	10.32 ± 0.44			1318.349
					1253.48	n,c,p	11.61 ± 0.61			1755.73
86	3012.06(13)	2^+,3^+	0.065(4)	8.86	2668.13		66.49 ± 1.30	5.1(19)E-4		344.28
					2257.22	n,c,p	7.65 ± 0.49			755.395
					1902.867	d,c,p	6.81 ± 1.30	9.2(17)E-4	$M1$	1109.193
					1096.6	n,p	10.06 ± 0.97			1915.687
					1000.41	n,p	3.96 ± 0.39			2011.65
					810.44	n,p	5.03 ± 0.58			2201.728
87	3042.30(5)	$0^+, 1^+, 2$	0.329(11)	8.13	2697.99	p	53.90 ± 1.15	5.3(10)E-4	$E2$,$M1$	344.28
					1932.94	c,p	10.99 ± 0.54	8.3(22)E-4	$M1$($E2$)	1109.193
					1727.72	c,p	22.31 ± 0.50	1.8(4)E-3		1314.635
					1436.67	p	12.80 ± 0.37			1605.584
88	3067.40(11)		0.033(2)	9.11	2312	n,c,p	94.20 ± 2.71			755.395
					1944.8	b,p	5.80 ±	> 4.9(17)E-2	($E0M1$)	1123.183
89	3074.86(16)		0.066(4)	8.68	1965.42	n,p	23.15 ± 1.34			1109.193
					1792.71	n,c,p	76.85 ± 5.76			1282.267
90	3079.64(18)	$3^+, 4^+$	0.091(5)	8.6	2324.32	c,p	38.02 ± 2.02	d	$M1$($E0$)	755.395
					1761.22	c,p	61.98 ± 3.48	6.2(19)E-3	$E2$($E1$)	1318.349

Table 3. Continued.

No.	E_i (keV)	I^π	I_β	log ft	E_γ (keV)	Type	$I_\gamma \pm \Delta I_\gamma$	$\alpha_K(\Delta\alpha_K)$	XL	E_f (keV)
91	3090.40(22)		0.009(1)	9.65	2335	n,p	100.0 ± 5.63			755.395
92	3098.99(8)		0.156(14)	8.33	2754.7	p	62.70 ± 1.21	4.1(9)E-4	$E2$,$M1$	344.28
					2168.44	d,c,p	33.17 ± 8.09			930.55
					500.23	n,p	4.13 ± 0.65			2598.784
93	3105.49(7)	2^+	0.057(2)	8.96	3105.45	n,p	19.11 ± 0.78			0
					2761.15	p	19.33 ± 0.78			344.28
					2350.3	n,c,p	25.56 ± 1.56			755.395
					805.84	n,p	36.0 ± 1.56			2299.636
94	3110.90(10)	$1^+,(2^+)$	0.087(3)	8.64	2495.53	c,p	100.0 ± 2.17	6.5(27)E-4	$M1(E2)$	615.373
95	3112.50(8)	$1^+,2^+$	0.120(8)	8.47	3112.27	n,p	2.14 ± 0.14			0
					2768.27	p	21.88 ± 0.53			344.28
					2182.1	n,c,p	20.88 ± 1.01	d	$M1$	930.55
					1171.19	p	31.26 ± 5.83			1941.157
					583	n,p	23.84 ± 2.12			2529.395
96	3140.17(7)	$1^+,2^+$	0.143(6)	8.39	3140.2	p	12.76 ± 0.31			0
					2795.92	p	46.08 ± 1.02	d	$E2$	344.28
					2209.71	n,p	22.24 ± 1.28			930.55
					1198.97	n,p	15.95 ± 1.33			1941.157
					874.85	n,p	2.97 ± 0.89			2264.833
97	3143.96(8)		0.060(2)	8.77	2799.81	p	18.76 ± 0.74			344.28
					2388.72	n,c,p	40.04 ± 1.26	d		755.395
					2020.67	n,p	20.02 ± 1.16	d	$E2$,$M1$	1123.183
					1022.73	n,p	21.18 ± 1.37			2121.061
98	3152.98(9)	$2^+,3,4^+$	0.056(10)	8.66	2808.61	6.96	3.68 ± 0.00	2.0(8)E-4	$E1(E2)$	344.28
					2043.787	t,c,p	68.97 ± 9.20		$(E2M1)$	1109.21
					1870.55	n	27.36 ± 3.68	d		1282.25
99	3214.23(9)		0.058(3)	8.55	1521.57	n,c,p	31.59 ± 3.27			1692.417
					1045.31	n,p	12.31 ± 1.63			2169.583
					887.32	n,p	56.10 ± 2.07			2325.928
100	3232.05(9)		0.068(3)	8.61	2887.52	n,p	22.50 ± 0.74	d	$E2$,$M1$	344.28
					2004.93	n,p	10.09 ± 0.83			1227.374
					1917.55	n,c,p	47.59 ± 1.20			1314.635
					1626.39	n,p	19.81 ± 1.67			1605.584
101	3236.92(9)	$2^+,3,4^+$	0.073(3)	8.58	2481.75	n,p	6.63 ± 0.96			755.395
					2306.15	c,p	36.82 ± 1.13			930.55
					911.73	n	17.02 ± 0.96			2325.928
					788.88	n,p	39.53 ± 1.57			2448.009
102	3285.12(7)	2^+	0.164(7)	8.14	2940.15	p	46.88 ± 0.99	3.9(11)E-4	$E2$,$M1$	344.28
					2162.05	n,c,p	21.01 ± 0.45			1123.183
					1970.49	c,p	32.11 ± 0.86			1314.635
					1343			> 8.0(8)E-2	$(E0M1)$	1941.157
103	3340.60(5)	3^-	0.118(6)	8.03	2996.26	p	23.19 ± 0.54			344.28
					2217.4	n,c,p	40.20 ± 1.02	d	$M1$	1123.183
					1424.76	n,p	10.31 ± 0.97			1915.687
					1075.87	n,c,p	26.30 ± 3.22			2264.833
104	3358.26(10)	2^+	0.074(10)	10.48	2602.85		86.21 ± 2.59	d	$E2$,$M1$	755.4
					2043.625	t,c,p	13.79 ± 3.45			1314.63

Notes: a) Energy of this peak is taken from [6]. b) Energy of this transition is taken from ICE measurements. n) New transition. d) Double transition, see table 5 [63]. t) Triple transition, see table 5 [63]. c) Transition is placed in the decay scheme on the basis of $\gamma\gamma$-coincidences. p) Transition is placed in the decay scheme on the basis of the balance of energies.

The log ft values listed there were calculated using the ^{152}Tb half-life of 17.5(1) h, decay energy Q_β = 3990(40) keV [51] and intensities of the ^{152}Gd level population. For some levels their intensity balances turned out to be negative and the condition $|I_{\beta i}| < \sigma(I_{\beta i})$ was satisfied. In those cases we gave only lower limits of log ft calculated under the assumption that $I'_{\beta i} = I_{\beta i} + 2\sigma(I_{\beta i})$.

6 Comparison of experimental and theoretical results

The nucleus $^{152}_{64}$Gd$_{88}$ has six neutrons more than the nearest doubly magic nucleus $^{146}_{64}$Gd$_{82}$, and the properties of its excited states should be described with allowance for the pairing force, which spherifies the nucleus, and for the

quadrupole force, which deforms it. Calculations of the Deformation Energy Surface (DES) of ^{152}Gd using the Pairing Plus Quadrupole model (PPQ) by Kumar and Gupta [40] suggested the shape of the nucleus. For an axially symmetrical nucleus they found that its potential energy had a minimum at $\beta = 0.19$ for the "prolate" shape, and $\beta = -0.04$ for a slightly"oblate" one. This fact suggests that the ^{152}Gd nucleus is quite soft with respect to vibrations, and possibly demonstrates shape coexistence.

A first determination of the ^{152}Gd low-energy levels was made by Zolnowski *et al.* [6]. They compared energies, spins, and parities of levels in the nucleus, as well as the reduced probabilities of their de-exciting transitions with those in the neighboring deformed ^{154}Gd, for which a detailed classification had been made by Meyer [69]. Besides the rotational bands built on the ground, β- and γ-vibrational states, he also identified such rotational bands on the octupole-vibrational and two-phonon (2β, $\beta\gamma$) states. The authors of [6] introduced this kind of "quasirotational" states in ^{152}Gd. Energies of the levels with negative parities in isotones with $N = 88$ were studied in [9] in comparison with the calculations taking into account Quadrupole-Octupole Coupling (QOC) of collective motion [70,71]. Good agreement between experimental and calculated values was observed for these levels. The reduced probabilities of the $E2$ transitions and the energies of the low-lying levels with positive parities were calculated in [9] in the framework of a microscopic model using the boson expansion technique and were compared with the experimental ones. The agreement was rather good, but the calculations of [40] of the PPQ model gave much better results for $B(E2)$ (despite the fact that the residual nucleon-nucleon interaction in both models was described similarly).

6.1 Q-phonon model, phase transitions models

Energies of rotational and quasirotational bands can be described by a number of phenomenological formulae, Bohr-Mottelson [72] equation, formulae of Ejiri [73] and Varshney [74]. Rotational and quasirotational spectra were described also in the framework of the model of the Variable Momentum of Inertia (VMI) [75–78] based on the cranking model [79]. The versions of the VMI differ from one another by the methods used for the calculation of the potential energy of the nucleus. Possible non-axiality of the nuclear shape was considered in [80, 81]. An approximate analytical solution for Hamiltonian eigenvalues of the asymmetric rotor was given in [81]. We used these models for the calculations of ^{152}Gd quasirotational level energies, see [82], but satisfactory agreement was not achieved.

Low-lying collective states of a nucleus can also be described in the framework of the Q-phonon [83] model, in which wave functions of excited states are created by applying the quadrupole operator to the wave function of the ground state. In this model, level energies in "quasirotational" bands are written as

$$E_I = \frac{IE(2_1^+)}{2} + \varepsilon_4 \frac{I(I-2)}{8} + \varepsilon_6 \frac{I(I-2)(I-4)}{48}\,. \quad (6)$$

With the Q-phonon approach, having measured experimental data on the reduced probabilities of $E2$ transitions $2_g^+ \to 0_g^+$, $4_g^+ \to 2_g^+$, $2_\gamma^+ \to 0_g^+$, $2_\gamma^+ \to 2_g^+$, one can easily calculate several shape invariants and thus gain important information on the structure of a given nucleus.

Lifetimes of the 2_g^+ and 4_g^+ states in ^{152}Gd are known, and on their basis it is possible to find the following quantities:

$$B(E2, 2_g^+ \to 0_g^+) = 0.349(18)\, e^2b^2 \quad \text{and}$$

$$B(E2, 4_g^+ \to 2_g^+) = 0.64(4)\, e^2b^2\,.$$

As the lifetime of the 2_γ^+ state is not known in this nucleus, the absolute probabilities of the $E2$ transitions $2_\gamma^+ \to 0_g^+$ $2_\gamma^+ \to 2_g^+$ can be evaluated by the formula [84]

$$B(E2, 2_\gamma^+ \to 0_g^+) \approx \frac{B(E2, 3_\gamma^+ \to 2_g^+)}{B(E2, 3_\gamma^+ \to 2_\gamma^+)} B(E2, 2_g^+ \to 0_g^+) =$$

$$\left(\frac{E_\gamma(3_\gamma^+ \to 2_\gamma^+)}{E_\gamma(3_\gamma^+ \to 2_g^+)}\right)^5 \times \frac{I_\gamma(3_\gamma^+ \to 2_g^+)\left(\frac{\delta^2}{1+\delta^2}\right)}{I_\gamma(3_\gamma^+ \to 2_\gamma^+)\left(\frac{\delta'^2}{1+\delta'^2}\right)}$$

$$\times B(E2, 2_g^+ \to 0_g^+)\,.$$

Afterwards, $B(E2, 2_\gamma^+ \to 2_g^+)$ can be calculated with the equation

$$B(E2, 2_\gamma^+ \to 2_g^+) = \left(\frac{E_\gamma(2_\gamma^+ \to 0_g^+)}{E_\gamma(2_\gamma^+ \to 2_g^+)}\right)^5$$

$$\times \frac{I_\gamma(2_\gamma^+ \to 2_g^+)}{I_\gamma(2_\gamma^+ \to 0_g^+)} \left(\frac{\delta^2}{1+\delta^2}\right) B(E2, 2_\gamma^+ \to 0_g^+)\,. \quad (7)$$

Substituting the experimental energies E_γ and intensities I_γ of the transitions de-exciting ^{152}Gd states and the mixture parameters of [24] in (7), we have

$$B(E2, 2_\gamma^+ \to 0_g^+) = 8.1(27) \times 10^{-4}\, e^2b^2 \quad \text{and}$$

$$B(E2, 2_\gamma^+ \to 2_g^+) = 5.2(24) \times 10^{-4}\, e^2b^2\,.$$

Following the receipt of [83], the reduced-probability ratios G, R_1 and W were found, as well as the relative $q(2_g^+)$ and absolute $\left|Q(2_g^+)\right|$ values of the quadrupole momenta of the

first-excited 2_g^+ state:

$$G = \frac{7}{10}\frac{B(E2, 4_g^+ \to 2_g^+)}{B(E2, 2_g^+ \to 0_g^+)} = 1.28(10)\,,$$

$$R_1 = \frac{B(E2, 2_\gamma^+ \to 0_g^+)}{B(E2, 2_g^+ \to 0_g^+)} = 2.3(8) \times 10^{-3}\,,$$

$$W = \frac{B(E2, 2_\gamma^+ \to 2_g^+)}{B(E2, 4_g^+ \to 2_g^+)} = 8(4) \times 10^{-3}\,,$$

$$q(2_g^+) = \frac{8}{7}\sqrt{\pi G(1 + R_1 - W)} = 2.28(13)\,,$$

$$\left|Q(2_g^+)\right| = q(2_g^+)\sqrt{B(E2, 2_g^+ \to 0_g^+)} = 1.35(9)\,.$$

Nuclear-shape invariants are introduced in the Q-phonon model as average scalars constructed of various numbers of quadrupole operators. Their values do not change under rotation of the coordinate system. In the geometric approach, the invariants are associated with the nuclear-shape parameters β and γ. The dependence of the shape invariants K_2–K_6 on the reduced probabilities of $E2$ transitions was determined by [85,86]

$$K_2 \equiv e_{\rm eff}^2 \langle 0_g^+ \left|(QQ)_0\right| 0_g^+\rangle \langle 0_g^+ \left|\beta^2\right| 0_g^+\rangle \approx B(E2, 0_g^+ \to 2_g^+) + B(E2, 0_g^+ \to 2_\gamma^+) \equiv K_2^{\rm appr} = 1.75(16)\, e^2 b^2\,,$$

$$K_3 \equiv \frac{\left|\langle 0_g^+ \left|(QQQ)_0\right| 0_g^+\rangle\right|}{\langle 0_g^+ \left|(QQ)_0\right| 0_g^+\rangle^{3/2}}\sqrt{5\sqrt{5}} = \sqrt{\frac{2}{35}}\frac{\langle 0_g^+|\beta^3 \cos 3\gamma|0_g^+\rangle}{\langle 0_g^+|\beta^2|0_g^+\rangle^{3/2}} \approx \sqrt{\frac{2G}{35}}\left[\left(\frac{1-R_1}{1+R_1}\right)\sqrt{1 - \frac{W}{1+R_1}} - \frac{2}{1+R_1}\sqrt{\frac{R_1 W}{1+R_1}}\right] \equiv K_3^{\rm appr} = 0.266(15)\,,$$

$$K_4 \equiv \frac{\left|\langle 0_g^+ \left|(QQ)_0^2\right| 0_g^+\rangle\right|}{\langle 0_g^+ \left|(QQ)_0\right| 0_g^+\rangle^2} = \frac{|\langle 0_g^+|\beta^4|0_g^+\rangle|}{\langle 0_g^+|\beta^2|0_g^+\rangle^2} \approx \frac{7}{10}\frac{B(E2, 4_g^+ \to 2_g^+)}{B(E2, 2_g^+ \to 0_g^+)} = G \equiv K_4^{\rm appr} = 1.28(10)\,.$$

If the effective charge is known, the average deformation parameter β^2 is governed by $K_2^{\rm appr}$ and its fluctuation by $K_4^{\rm appr} - 1$. Similarly, the effective value of γ is found as $\gamma_{\rm eff} = \frac{1}{3}\arccos\left(\sqrt{\frac{35}{2}}K_3^{\rm appr}\right)$, but since only the absolute value of $K_3^{\rm appr}$ was found by us, it is impossible to discriminate between $\gamma_{\rm eff}$ and $\frac{\pi}{3} - \gamma_{\rm eff}$. On the basis of $\sqrt{\frac{35}{2}}K_3^{\rm appr} = 1.11(6)$ calculated for ^{152}Gd, one can conclude that $\gamma^{\rm eff} \approx 0°$ or $60°$.

Table 4. Comparison of the experimental ^{152}Gd level energies to calculated ones up to $I^\pi = 14^+$.

I^π	E (exp) (keV)	σ (E) (keV)	E (cal) (keV)
2	344.3	0.5	344.3
4	755.4	0.5	756.6
6	1227.4	0.5	1226.7
8	1746.8	0.5	1745.2
10	2300.4	0.8	2302.4
12	2883.8	1.1	2888.5
14	3499.2	1.5	3494.0

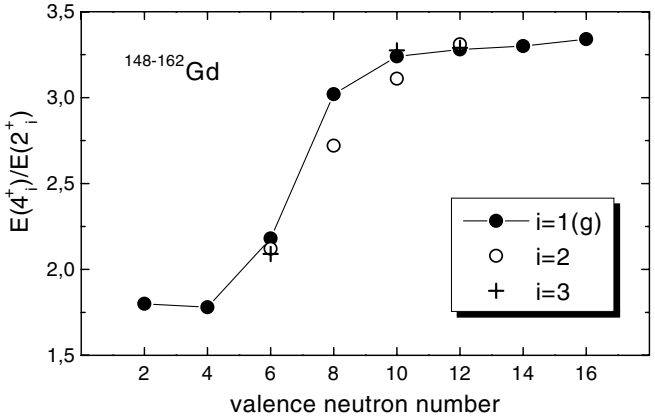

Fig. 5. Ratios $R_{4/2}^i = E(4_i^+)/E(2_i^+)$ for the even Gd isotopes.

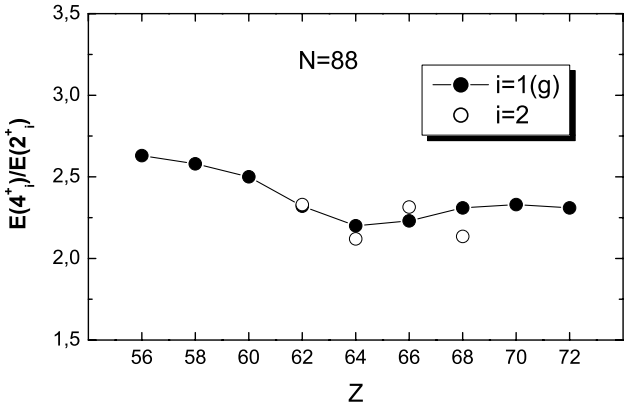

Fig. 6. Ratios $R_{4/2}^i = E(4_i^+)/E(2_i^+)$ for the even $N = 88$ isotones.

In this work, for comparison of the experimental and theoretical level energies of the ^{152}Gd yrast band, the dependence given by eq. (6) was used.

The results of the fit are shown in table 4. The values of the fitted parameters are $\varepsilon_4 = 67.7$ keV and $\varepsilon_6 = -9.67$ keV. The averaged residual of the level energies $\langle|E_{\rm exp} - E_{\rm calc}|\rangle = 2.21$ keV. That analysis was also performed with allowance for the level $I^\pi = 16^+$, whose experimental level energy is unreliable. Including it into the yrast band worsened the average residual of (6) from 2.21 keV to 4.05 keV, almost by twofold. The energy ratio of the 4_g^+ and 2_g^+ levels in the ^{152}Gd nucleus indicates

Table 5. Experimental and theoretical level energy ratios for ^{152}Gd.

	$R_{4/2}$	$R_{6/2}$	$R_{8/2}$	$R_{10/2}$	$R_{12/2}$	$R_{14/2}$	$\frac{E(0_2^+)}{E(2_1^+)}$	$\frac{E(0_3^+)}{E(2_1^+)}$	$\frac{E(0_4^+)}{E(2_1^+)}$
^{152}Gd(exp)	2.194	3.565	5.074	6.682	8.376	10.164	1.787	3.043	
$E(5)$	2.199	3.590	5.169	6.934	8.881	11.009	3.03		7.5
$X(5)$	2.904	5.430	8.483	12.027	16.041	20.514	5.67	14.1	

Table 6. Experimental and theoretical reduced-probability ratios for ^{152}Gd

	$\frac{B(E2,4_g^+\to 2_g^+)}{B(E2,2_g^+\to 0_g^+)}$	$\frac{B(E2,6_g^+\to 4_g^+)}{B(E2,2_g^+\to 0_g^+)}$	$\frac{B(E2,0^+\to 2_g^+)}{B(E2,2_g^+\to 0_g^+)}$	$\frac{B(E2,2_\beta^+\to 0_3^+)}{B(E2,2_g^+\to 0_g^+)}$
^{152}Gd(exp)	1.83(15)	2.72(56)	2.46(53)	0.49
E(5)	1.68	2.21	0.86	0.75
X(5)	1.58	1.98	0.63	0.79

that it belongs to the transitional region. In figs. 5 (6) the values of $R^i_{4/2} = E(4_i^+)/E(2_i^+)$ for even Gd isotopes (even $N = 88$ isotones) are shown. The index $i = 1$ denotes the ground-state band, $i = 2(3)$ stand for bands built on the second (third) 0^+ state. For ^{152}Gd $R^1_{4/2} = 2.1$, and this fact suggests the probable position of the nucleus at the critical point of either the first-order phase transition from the vibrator to the γ-unstable ($U(5)$–$SO(6)$) shape, or the second-order phase transition from the vibrator to the deformed ($U(5)$–$SU(3)$) shape. A theory for the calculation of the properties of nuclei close to the critical point of the former ($E(5)$ symmetry) and the latter ($X(5)$ symmetry) was recently proposed by F. Iachello [87,88]. He points out that there is a new class of dynamic symmetries describing systems undergoing phase transitions, based not on the group-theoretical description but on "representation symmetries" associated with the zeros of special functions. For the Bohr Hamiltonian

$$H = -\frac{\hbar^2}{2B}\left[\frac{1}{\beta^4}\frac{\partial}{\partial\beta}\beta^4\frac{\partial}{\partial\beta} + \frac{1}{\beta^2\sin 3\gamma}\frac{\partial}{\partial\gamma}\sin 3\gamma\frac{\partial}{\partial\gamma} - \frac{1}{4\beta^2}\sum_k \frac{Q_k^2}{\sin^2(\gamma - \frac{2}{3}\pi k)}\right] + V(\beta,\gamma)\,,$$

where the potential is taken to be a square well in the variable β and a harmonic oscillator in γ for the $X(5)$ symmetry, and depends only on β for the $E(5)$, one can obtain the Bessel equation

$$\varphi'' + \frac{\varphi'}{z} + \left[1 - \frac{\nu^2}{z^2}\right]\varphi = 0\,,$$

where $\varphi(\beta) = \beta^{3/2} f(\beta)$, $z = \beta k$.

In this case, the energy eigenvalues are fixed by the symmetry and can be expressed in terms of the zeros of the Bessel function J_ν, with no free parameters at all:

$$\nu = \tau + \frac{3}{2}, \quad \text{for the } U(5)\text{–}SO(6) \text{ transition, or} \qquad (8)$$

$$\nu = \left(\frac{L(L+1)}{3} + \frac{9}{4}\right)^{1/2}, \quad \text{for } U(5)\text{–}SU(3)\,. \qquad (9)$$

For instance, the energy of the transition $4_g^+ \to 2_g^+$ given in units of the $2_g^+ \to 0_g^+$ transition is defined as

$$R_{4/2} = \frac{E_{4_{1,2}} - E_{0_{1,0}}}{E_{2_{1,1}} - E_{0_{1,0}}} = \frac{\kappa^2_{1,2} - \kappa^2_{1,0}}{\kappa^2_{1,1} - \kappa^2_{1,0}}\,,$$

where $E_{L_{\xi,\tau}}$ stands for the energy of a level with spin L, determined as the ξ-th zero of the Bessel function J of the ν-th order (ν is found using (8) or (9)), and $\kappa_{\xi,\tau}$ is the ξ-th zero of the function J_ν. Comparison of the experimental $R_{I/I-2}$ of ^{152}Gd with their theoretical values calculated in [87] and [88] is given in table 5. Reduced-probability ratios calculated in the papers cited above for some of the $E2$ transitions and their experimental values for ^{152}Gd are shown in table 6. The calculations were also carried out without a free parameter. The results of the comparison for $B(E2)$ show preference for neither the $E(5)$ nor the $X(5)$ symmetry, although the calculated data for $E(5)$ are a little closer to the experimental ones. On the other hand, the experimental $R_{I/I-1}$ almost coincide with the calculated ones if $E(5)$ symmetry is assumed and significantly differ from them in the case of $X(5)$. Also, the ratio $E(0_2^+)/E(2_1^+)$ calculated for the $E(5)$ symmetry is very close to its experimental value for $E(0_3^+)/E(2_1^+)$ (see table 5).

In this connection a question arises as to the nature of the quasirotational band built on the first-excited 0^+ state of ^{152}Gd and its possible "intruder" origin. This fact spurred us to perform various calculations in the framework of the IBA-2 model under different assumptions of the nature of this state. The fact that $(R_{I/I-2})_{\rm exp}$ is close to its theoretical values for the $E(5)$ symmetry seems to be rather unpredictable and points out the complexity of the transition from the spherical to the deformed nuclear shape.

6.2 Interacting-Boson Model (IBA)

Energies of the quasirotational bands and transition properties ($B(E2)$, $\rho(E0)$, $X(E0/E2)$) were calculated in [10]

by the projection model and IBA-1. The comparison showed that both models reproduced the level energies quite well, the reduced probabilities of the $E2$ transitions satisfactorily, and those for $E0$ transitions unsatisfactorily. The IBA-1 model with seven parameters was used in [23] for the description of electromagnetic properties of five $N = 88$ nuclei with the same set of parameters employed for all of them. Several nuclei were analyzed in [22] in the $U(5)$ limit of IBA-1. The excitation energy ratios of ^{152}Gd $R^{\rm calc}_{4/2} = 2.03$ ($R^{\rm exp}_{4/2} = 2.19$), and the reduced transition probability ratios were found to be $\frac{B(E2,4^+\to 2^+)}{B(E2,2^+\to 0^+)} = 1.83$ (calculated) and 1.9 (experimental). In spite of such good agreement for the 2^+_g and 4^+_g levels, the authors of [22] concluded that the ^{152}Gd nucleus cannot be considered as only vibrational as the predicted excitation energy of the 0^+_3 level was 1425 keV, while the observed one was 1047.77 keV. In this case this level could be the head level of the "intruder" band, but 0^+ states with energy higher than 1048 keV were observed no more.

An extensive analysis of the ^{152}Gd properties within the proton-neutron Interacting-Boson Model (IBA-2) has been made in [24]. The Hamiltonian has been used in the simplified form with nine parameters,

$$H = \varepsilon(\hat{n}_{d\nu} + \hat{n}_{d\pi}) + \kappa Q_\nu Q_\pi + V_{\pi\pi} + M_{\nu\pi}\,,$$

where

$$\hat{n}_{d\rho} = d^+_\rho \cdot \tilde{d}_\rho\ .$$

is the operator of the d-boson number for protons ($\rho = \pi$) or neutrons ($\rho = \nu$).
The quadrupole operator Q_ρ has the form

$$Q_\rho = (d^+_\rho\ \tilde{s}_\rho + s^+_\rho\ \tilde{d}_\rho)^{(2)} + \chi_\rho (d^+_\rho\ \tilde{d}_\rho)^{(2)}\,, \qquad \rho = \pi, \nu\,.$$

The Majorana operator is

$$M_{\nu\pi} = \frac{1}{2}\xi_2 (s^+_\nu d^+_\pi - d^+_\nu s^+_\pi)^{(2)} (\tilde{s_\nu} \tilde{d_\pi} - \tilde{d_\nu} \tilde{s_\pi})^{(2)} - \sum_{k=1,3} \xi_k (d^+_\nu d^+_\pi)^{(k)} (\tilde{d_\nu} \tilde{d_\pi})^{(k)}\,,$$

and the interaction between π-π bosons is

$$V_{\pi\pi} = \frac{1}{2} \sum_{L=0,2} \sqrt{2L+1} C^\pi_L (d^+_\pi d^+_\pi)^{(L)} (\tilde{d_\pi} \tilde{d_\pi})^{(L)}\,.$$

The IBA-2 calculations along the lines of [24] are denoted as Version I below.

Even if the overall fit with Version I is rather good, some problems have been noticed in [24]. Particularly, the energies of the 0^+_3 and 2^+_4 levels are not reproduced. The energy of the latter level is improved in [24] with the modified parameters of the Majorana force thus lowering the position of the mixed-symmetry 2^+ state.

The situation with the calculated energies of the 0^+ states, however, evokes the suggestion of ref. [22] that some of the low-lying 0^+ states might be of "intruder" character giving rise to the whole "intruder" band. We inspect this possibility within the extended IBA-2 model in which the intruder s'_π-boson is added to the IBA-2 space. We choose the intruder boson in the proton sector, since it corresponds to the interpretation of the intruder state as a proton excitation in the vicinity of the $Z = 64$ shell. The simple treatment of the intruder boson is considered with the single boson energy $\varepsilon_{s'_\pi} \hat{n}_{s'_\pi}$ added to the IBA-2 Hamiltonian. The interaction between the intruder s'_π-boson and the d_π-boson is managed by the term

$$\alpha (d^+_\pi\ \tilde{s'_\pi} + s'^+_\pi\ \tilde{d}_\pi)^{(2)}$$

added to the proton quadrupole operator Q_π. Note that we consider the total boson number conserving the Hamiltonian. The alternative treatment in which the intruder boson brings about a change of the total boson number [89] is essentially equivalent to the present approach bringing mainly some renormalization of the parameters $\varepsilon_{s'_\pi}$ and α.

We discuss two variants of the extended IBA-2 model. In calculations denoted as Version II below, the intruder state is identified with the 615.37 keV (0^+) level. In calculations of Version III, the intruder state is connected to the 1047.77 keV (0^+) excitation. We also compare the analytical expression of the vibrational $SU(5)$ limit of the IBA-1,

$$E_{\rm cal} = a_1 n_d + a_2 n_d (n_d + 4) + a_3 v(v+3) + a_4 I(I+1)$$

with the measured energies (Version IV). The best fit to the free parameters gave the following values : $a_1 = 383.3$, $a_2 = -7.0061$, $a_3 = 11.2508$, and $a_4 = 1.8721$.

The respective parameters used in our calculations are shown in tables 7 and 8. In Version I, the Hamiltonian parameters of [24] are employed, whereas effective e_2 charges are slightly changed as compared to [24].

Table 7. The IBA-2 parameters for ^{152}Gd.

Version	ϵ	κ	χ_π	χ_ν	C^π_0	C^π_2
I	0.73	−0.07	−2.0	−0.4	−0.2	−0.1
II	0.74	−0.12	−0.60	−0.54	0	0
III	0.69	−0.06	−1.95	−0.40	−0.2	−0.1

Version	ξ_1	ξ_2	ξ_3	$\varepsilon_{s'_\pi}$	α
I	0.25	0.25	0.25	0	0
II	0.3	0.05	0.3	0.01	0.60
III	0.25	0.25	0.25	0.90	0.90

Table 8. The IBA-2 charges for ^{152}Gd.

Version	$e2_\pi$	$e2_\nu$	$e0_\pi$	$e0_\nu$
I	0.12703	0.05828	−0.00132	−0.00026
II	0.12129	0.11322	−0.00224	0.00195
III	0.17347	−0.16012	−0.00738	0.02374

Table 9. Calculated and experimental energies in Version I, Version II, Version III —IBA-2 calculations, and in Version IV —$SU(5)$ limit.

	E(exp)	$\sigma(E$(exp))	Version I	Version II	Version III	Version IV
0_2^+	615.4	0.5	633.4	539.2	582.8	683.5
0_3^+	1047.8	0.5	1411.3	1070.9	1000.4	
2_1^+	344.3	0.5	314.7	279.6	334.2	405.0
2_2^+	930.6	0.5	934.0	887.7	870.6	807.3
2_3^+	1109.2	0.5	1195.3	1039.4	1105.3	1060.5
2_4^+	1318.4	0.5	1752.4	1546.6	1408.5	
3_1^+	1434.0	0.5	1489.0	1543.0	1407.4	1229.3
4_1^+	755.4	0.5	723.6	723.6	740.3	833.5
4_2^+	1282.3	0.5	1420.1	1379.4	1337.6	1244.2
4_3^+	1550.2	0.5	1751.1	1624.6	1631.3	1663.5
5_1^+	1861.6	0.5	2029.4	2207.0	1924.9	
6_1^+	1227.4	0.5	1229.4	1303.2	1227.9	1285.4
6_2^+	1668.1	0.5	1979.6	1995.3	1871.2	1704.7
$\langle\|E(\text{exp}) - E(\text{cal})\|\rangle$			142.0	120.0	53.0	75.7

Note: Here indices are the order numbers of the levels ordered with increasing energies. In the tables below, indices "g" stand for 2_1^+, 4_1^+, and 6_1^+, and indices "γ" for 2_3^+, 3_1^+, 4_3^+, 5_1^+, and 6_3^+ in all the versions, while the indices "β" stand for the 0_3^+, 2_4^+, 4_4^+, and 6_4^+ in the case of Version II, but for 0_2^+, 2_2^+, 4_2^+, and 6_2^+ in Version III.

Table 10. Comparison of experimental and calculated absolute $B(E2)$ values (in e^2b^2) for ^{152}Gd.

	$2_g^+ \to 0_g^+$	$4_g^+ \to 2_g^+$	$6_g^+ \to 4_g^+$	$2_\beta^+ \to 0_\beta^+$	$2_\beta^+ \to 0_g^+$	$2_\beta^+ \to 2_g^+$	$2_\beta^+ \to 4_g^+$	$0_\beta^+ \to 2_g^+$	$2_\gamma^+ \to 0_g^+$
Experiment	0.349(18)	0.64(4)	0.95(19)	0.171(14)	0.00138(11)	0.084(7)	0.096(8)	0.86(18)	
IBA-2, Version I	0.2403	0.4643	0.5911	0.2186	0.0015	0.0871	0.1316	0.4844	0.0025
IBA-2, Version II	0.3692	0.5639	0.6485	0.2247	0.0007	0.0033	0.0051	0.0068	0.0125
IBA-2, Version III	0.1188	0.2873	0.4149	0.1451	0.0011	0.0731	0.1762	0.5030	0.0016

Table 11. $B(E2)$ branching ratios for transitions from the β-band of ^{152}Gd.

	$E_{\text{lev}}(4_\beta^+) = 1282.27$ keV			$E_{\text{lev}}(6_\beta^+) = 1668.1$ keV
	$\frac{4_\beta^+ \to 2_g^+}{4_\beta^+ \to 4_g^+}$	$\frac{4_\beta^+ \to 6_g^+}{4_\beta^+ \to 4_g^+}$	$\frac{4_\beta^+ \to 2_\beta^+}{4_\beta^+ \to 4_g^+}$	$\frac{6_\beta^+ \to 4_\beta^+}{6_\beta^+ \to 6_g^+}$
Experiment	0.0346(15)	< 6000	6.67(22)	16.6*
IBA-2, Version I	0.001	2.178	6.815	14.327
IBA-2, Version II	0.558	2.984	185.229	274.477
IBA-2, Version III	0.083	3.240	4.234	8.581

Experimental and calculated energies and electromagnetic properties are compared in tables 9 to 16. Experimental level energies, γ-ray energies and intensities and total intensities of transitions in ^{152}Gd are taken from this paper. Reduced-probability ratios are calculated by eq. (7) with the mixture parameters δ taken from [24]. Measured level lifetimes $T_{1/2}^{\text{lev}}$ for the calculation of the absolute experimental $B(E2)$ $[e^2b^2]$ are extracted from [13] :

$$B(E2, I_i \to I_f) = 81.61 \times \frac{\ln 2}{T_{1/2}^{\text{lev}}} \frac{I_\gamma(I_i \to I_f)}{E_\gamma^5 \sum_{k=1}^{i-1} I_{ik}^{\text{tot}}} \times \frac{\delta^2}{1+\delta^2}\,,$$

where E_γ is in keV. In order to estimate the difference between the calculated and experimental results, we determine the averaged residuals as

$$\bar{x} = \sum_{i=1}^{n} \frac{1}{n} \frac{|x_{\text{exp}}(i) - x_{\text{theo}}(i)|}{x_{\text{exp}}(i)}\,, \qquad (10)$$

where $x_{\text{exp}}(i)$ ($x_{\text{theo}}(i)$) stands for the i-th experimental (calculated) value represented in tables 11 to 15.

None of the calculations explains experimental data in a completely satisfactory way. The smallest discrepancies

Table 12. $B(E2)$ branching ratios for transitions from the γ-band of ^{152}Gd.

	$E_{\rm lev}(2^+_\gamma) = 1109.19$ keV				$E_{\rm lev}(3^+_\gamma) = 1434.02$ keV		
	$\frac{2^+_\gamma \to 0^+_g}{2^+_\gamma \to 2^+_g}$	$\frac{2^+_\gamma \to 4^+_g}{2^+_\gamma \to 2^+_g}$	$\frac{2^+_\gamma \to 0^+_\beta}{2^+_\gamma \to 0^+_g}$	$\frac{2^+_\gamma \to 2^+_\beta}{2^+_\gamma \to 2^+_g}$	$\frac{3^+_\gamma \to 2^+_g}{3^+_\gamma \to 4^+_g}$	$\frac{3^+_\gamma \to 2^+_\beta}{3^+_\gamma \to 2^+_g}$	$\frac{3^+_\gamma \to 2^+_\gamma}{3^+_\gamma \to 2^+_g}$
Experiment	2.5(6)	8.4(19)	3.18(9)	108(25)	0.375(14)	3.41(12)	19.9(10)
IBA-2, Version I	0.544	13.027	22.059	76.071	0.314	11.73	66.682
IBA-2, Version II	0.066	0.004	0.129	0.024	0.32	0.147	14.901
IBA-2, Version III	36.868	1709.847	26.454	5386.942	0.034	122.783	705.040

	$E_{\rm lev}(4^+_\gamma) = 1550.15$ keV			$E_{\rm lev}(5^+_\gamma) = 1861.7$ keV		
	$\frac{4^+_\gamma \to 4^+_g}{4^+_\gamma \to 2^+_g}$	$\frac{4^+_\gamma \to 2^+_\gamma}{4^+_\gamma \to 2^+_g}$	$\frac{4^+_\gamma \to 3^+_\gamma}{4^+_\gamma \to 2^+_\gamma}$	$\frac{5^+_\gamma \to 6^+_g}{5^+_\gamma \to 4^+_g}$	$\frac{5^+_\gamma \to 4^+_\beta}{5^+_\gamma \to 4^+_g}$	$\frac{5^+_\gamma \to 3^+_\gamma}{5^+_\gamma \to 4^+_g}$
Experiment	12.5(6)	62(4)	8000(?)	5.4(5)*	2.00(20)*	38(3)*
IBA-2, Version I	3.632	265.556	0.923	5.725	7.014	136.597
IBA-2, Version II	199.628	445.319	0.583	7.078	0.101	29.781
IBA-2, Version III	0.117	121.821	1.172	1499.288	1830.954	46381.557

Table 13. $B(E2)$ branching ratios for transitions from the 2γ-band of ^{152}Gd.

	$E_{\rm lev}(2^+_5) = 1605.58$ keV						
	$\frac{2^+_5 \to 0^+_g}{2^+_5 \to 2^+_g}$	$\frac{2^+_5 \to 4^+_g}{2^+_5 \to 2^+_g}$	$\frac{2^+_5 \to 0^+_\beta}{2^+_5 \to 0^+_g}$	$\frac{2^+_5 \to 0^+_\beta}{2^+_5 \to 2^+_\beta}$	$\frac{2^+_5 \to 2^+_\beta}{2^+_5 \to 2^+_g}$	$\frac{2^+_5 \to 2^+_\gamma}{2^+_5 \to 2^+_g}$	$\frac{2^+_5 \to 2^+_\beta}{2^+_5 \to 2^+_\gamma}$
Experiment	≥ 7.4	≥ 24	36(6)	0.24(6)	≥ 1110	≥ 1720	0.65(17)
IBA-2, Version I	1.135	2.604	6.332	0.698	10.291	13.536	0.76
IBA-2, Version II	0.666	12.261	11.033	0.045	163.387	21.764	7.507
IBA-2, Version III	0.514	2.514	5.911	0.488	6.225	91.883	0.068

	$E_{\rm lev}(2^+_5) = 1605.58$ keV			$E_{\rm lev}(3^+_2) = 1839.70$ keV			
	$\frac{2^+_5 \to 0^+_3}{2^+_5 \to 0^+_g}$	$\frac{2^+_5 \to 0^+_3}{2^+_5 \to 0^+_\beta}$	$\frac{2^+_5 \to 0^+_3}{2^+_5 \to 2^+_g}$	$\frac{3^+_2 \to 2^+_g}{3^+_2 \to 4^+_g}$	$\frac{3^+_2 \to 2^+_g}{3^+_2 \to 2^+_\beta}$	$\frac{3^+_2 \to 2^+_g}{3^+_2 \to 2^+_\gamma}$	$\frac{3^+_2 \to 2^+_\beta}{3^+_2 \to 2^+_\gamma}$
Experiment	64(9)	1.79(18)	≥ 470	0.47(12)	0.069(4)	0.096(20)	1.39(28)
IBA-2, Version I	1841.103	290.739	2089.821	0.057	0.077	0.015	0.195
IBA-2, Version II	54.087	4.902	36.032	0.855	0.025	0.128	5.179
IBA-2, Version III	2.873	0.486	1.477	11.634	46.437	0.186	0.004

	$E_{\rm lev}(3^+_2) = 1839.70$ keV		
	$\frac{3^+_2 \to 2^+_4}{3^+_2 \to 2^+_5}$	$\frac{3^+_2 \to 2^+_4}{3^+_2 \to 2^+_\beta}$	$\frac{3^+_2 \to 4^+_\beta}{3^+_2 \to 2^+_\beta}$
Experiment		≤ 1.2	3.6(7)
IBA-2, Version I	0.209	1522.577	12.783
IBA-2, Version II	0.184	3.726	5.975
IBA-2, Version III	0.008	32.228	35.143

between the experimental and theoretical energies are obtained for Version III. The averaged residuals for 18 values of $B(E2)$, $\rho(E0)$, and $X(E0/E2)$ do not exceed 60% for Versions I and II, whereas for Version III they are approximately two times as large. The values of $\bar{x}$ for the $B(E2)$ ratios of transitions de-exciting the quasirotational bands were found to be significantly larger in Versions I and II (3500% and 2600%), and the largest (9400%) in Version III. In the latter case large residuals were obtained for transitions from all bands except the β-band. The analysis shows that preference should be given to Versions I and II rather than to Version III. Note, however, that in Version II, the experimental $B(E2)$ value for the crucial $0^+_\beta \to 2^+_g$ transition is quite large and in contradiction to the small

Table 14. Experimental and theoretical $\rho(E0)$ values of ^{152}Gd. All quantities have been multiplied by 100.

	$\rho(E0)$ for transition								
$I_i^\pi \to I_f^\pi$	$0_\beta^+ \to 0_g^+$	$2_\beta^+ \to 2_g^+$	$4_\beta^+ \to 4_g^+$	$0_3^+ \to 0_g^+$	$0_3^+ \to 0_\beta^+$	$2_4^+ \to 2_g^+$	$2_4^+ \to 2_\beta^+$	$2_5^+ \to 2_g^+$	$2_5^+ \to 2_\beta^+$
E_γ (keV)	615.6	586.27	526.85	1047.9	432.5	974.05	387.80	1261.32	675.01
Experiment	6.6(14)	4.6(4)							
IBA-2, Version I	3.79	3.12	3.66	0.0000	6.47	0.0000	4.06	0.002	0.027
IBA-2, Version II	0.05	0.14	0.25	3.84	0.31	7.57	0.6	1.42	0.03
IBA-2, Version III	18.36	1.48	2.19	0.01	0.02	1.14	3.44	1.77	0.43

Table 15. Experimental and theoretical $X(E0/E2)$ values of ^{152}Gd. All quantities have been multiplied by 100.

	$X(E0/E2)$ for transition							
$I_i^\pi \to I_f^\pi$	$2_\beta^+ \to 2_g^+$	$4_\beta^+ \to 4_g^+$	$0_3^+ \to 0_g^+$	$0_3^+ \to 0_\beta^+$	$2_4^+ \to 2_g^+$	$2_4^+ \to 2_\beta^+$	$2_5^+ \to 2_g^+$	$2_5^+ \to 2_\beta^+$
E_γ (keV)	586.27	526.85	1047.9	432.5	974.05	387.80	1261.32	675.01
Experiment	6.8(5)	24.2(19)	6.9(7)	2.25(23)		36(8)		
IBA-2, Version I	6.03	12.95	6.92	3.62	0.34	102.45	135.41	181.6
IBA-2, Version II	7.19	22.12	3.9	2.8	8462.24	2.45	310.14	0.04
IBA-2, Version III	3.42	7.5	6.96	0.03	38471.37	415.06	366.77	14.32

Table 16. Average parameters, calculated with eq. (10).

Model	$B(E2)$		$B(E2)$ branching ratios								$\rho(E0)$		$X\left(\frac{E0}{E2}\right)$	
			γ-band		2γ-band		β-band		0_3^+-band					
	$\bar{x}$	n	$\bar{x}$	n	$\bar{x}$	n	$\bar{x}$	n	$\bar{x}$	n	$\bar{x}$	n	$\bar{x}$	n
IBA-2, Version I	0.34	8	1.74	13	91.99	16	0.54	4	7.68	12	0.38	2	0.61	5
IBA-2, Version II	0.52	8	2.23	13	1.59	16	14.60	4	89.30	12	0.98	2	0.39	5
IBA-2, Version III	0.44	8	212	13	46.35	16	0.80	4	59.70	12	1.23	2	2.54	5
Tagziria [24],IBA-2	0.37	8												
Tagziria [24], DDM	0.52	7												
Kumar [40], PPQ	4.31	3	0.66	13	5.01	15	0.52	4	1.01	9	2.51	2	0.52	3
Lipas [10], IBA-1	0.06	2	0.50	4			1.14	2			2.63	2	0.25	2
Lipas [10], PMI	3.19	2	1.56	4			7.90	2			2.64	2	4.66	2
Lipas [10], PMA	2.51	2	1.60	4			10.02	2						
Zolnowski [9], BE6			0.84	12			0.59	3	0.92	1				

calculated one. The interpretation of the 615.37 keV (0^+) level as the intruder state is not thus much supported.

7 Conclusion

The decay of ^{152}Tb has been investigated by measuring single γ-rays as well as $\gamma\gamma$-coincidences with the use of HPGe detectors. Out of the 704 transitions observed, 347 were identified as belonging to the decay of the ^{152}Gd excited states for the first time, 242 transitions were placed into the ^{152}Tb $\longrightarrow$ ^{152}Gd decay scheme, 131 of them for the first time. Also, among the 111 levels introduced into the decay scheme, 46 are new. Using the more precise and full data on the intensities of γ-transitions, and previously reported conversion electron intensities, the $E0$ or $E0 + M1$ multipolarities were suggested for several transitions. For a number of low-lying levels the electron capture to positron decay ratio was found. For most of the levels, their spins and parities were determined, as well as $\log ft$ for β-transitions to these levels from ^{152}Tb.

As a result of the comparison performed in this work, we found that the best description of experimental energies of the yrast band levels in ^{152}Gd can be obtained in the framework of the Q-phonon model. Level energy ratios within the yrast band $R_{I/2}$ were found to be rather close to the calculations for the first-order ($E(5)$) phase transitions at the critical point [87,88], carried out without free parameters.

Absolute reduced probabilities and their ratios for the transitions within and outside quasirotational bands were best described with the PPQ [40] model (see tables 7–18 in [82]). Within the IBA-2 model, the agreement observed for level schemes I and II was better for reduced probabilities and worse in the case of level energies than for level scheme III.

J.D. acknowledges support from GACR Grant No. 202/99/0149 and 202/02/0939. V.S.P. is thankful to Prof. N. Severijns and his colleagues for fruitful discussions and kind hospitality during his visit to the Katholieke Universiteit Leuven, Belgium. This work was partially supported by the Russian Foundation for Basic Research.

References

1. Agda Artna-Cohen, Nucl. Data Sheets **79**, 1 (1996).
2. R.A. Meyer, Fizika (Zagreb) **22**, 153 (1990).
3. N.M. Stewart *et al.*, Z. Phys. A**335**, 13 (1990).
4. J. Goswamy *et al.*, Appl. Radiat. Isot., **4-2**, 1025 (1991).
5. K.P. Artamonova *et al.*, Izv. Akad. Nauk SSSR, Ser. Fiz., **43**, 935 (1979).
6. D.R. Zolnowski, E.G. Funk, J.W. Mihelich, Nucl. Phys. A **177**, 513 (1971).
7. J. Adam *et al.*, Izv. Akad. Nauk SSSR, Ser. Fiz. **34**, 813 (1970).
8. I. Tago, Y. Kawase, K. Okano, A **335**, 477 (1990).
9. D.R. Zolnowski *et al.*, Phys. Rev. C **21**, 2556 (1980).
10. P.O. Lipas *et al.*, Phys. Scr. **27**, 8 (1983).
11. M. Guttormsen *et al.*, Phys. Scr. **22**, 210 (1980).
12. Y. Gono, J. Phys. Soc. Jpn. **29**, 543 (1970).
13. N.R. Johnson *et al.*, Phys. Rev. C **26**, 1004 (1982).
14. D.G. Fleming *et al.*, Phys. Rev. C **8**, 806 (1973).
15. R. Bloch, B. Elbek, P.O. Tjom, Nucl. Phys. A **91**, 576 (1967).
16. M. Asai *et al.*, Japan Atomic Energy Research Institute, Takasaki Ion Accelerators for Advanced Radiation Applications, Annu. Rep., 1994, (1995) p. 184.
17. N.A. Matt *et al.*, Phys. Rev. C **59** (1999) 665.
18. K. Blaum *et al.*, Eur. Phys. J. D **11**, 37 (2000).
19. A. Arima, F. Iachello, Ann. Phys. (N.Y.) **281**, 2 (2000).
20. A.M. Demidov *et al.*, Yad. Fiz. **60**, 581 (1997); Phys. At. Nucl. **60**, 503 (1997).
21. Y.M. Zhao, Y. Chen, Phys. Rev. C **52**, 1453.
22. J. Kern *et al.*, Nucl. Phys. A **593**, 21 (1995).
23. A. Gómez, O. Castanõs, A. Frank, Nucl. Phys. A **589**, 267 (1995).
24. H. Tagziria *et al.*, J. Phys. G **16**, 1323 (1990).
25. Y. Ha, D. Fu, Chin. J. Nucl. Phys. **12**, 151 (1990).
26. C.S. Han, D.S. Chuu, S.T. Hsieh, Phys. Rev. C **42**, 280 (1990).
27. O. Engel *et al.*, Nucl. Phys. A **515**, 31 (1990).
28. P.O. Lipas, P. Toivonen, E. Hammaren, Nucl. Phys. A **469**, 348 (1987).
29. J. Dobes, Nucl. Phys. A **469**, 424 (1987).
30. K. Zajac, S. Szpikowski, Acta Phys. Pol. B **17**, 1109 (1986).
31. P.O. Lipas, P. Toivonen, D.D. Warner, Phys. Lett. B **155**, 295 (1985).
32. K. Heyde, P. Van Isaker, J. Jolie, Hyperfine Interact. **22**, 339 (1985).
33. C.S. Han *et al.*, Phys. Lett. B **163**, 295 (1985).
34. R.F. Casten, W. Frank, P. von Brentano, Nucl. Phys. A **444**, 133 (1985).
35. A.B. Balantekin, B.R. Barrett, Phys. Rev. C **32**, 288 (1985).
36. M. Sambataro *et al.*, Nucl. Phys. A **423**, 333 (1984).
37. D.S. Chuu *et al.*, Phys. Rev. C **30**, 1300 (1984).
38. A. Arima, F. Iachello, Ann. Phys. (N.Y.) **99**, 253 (1976).
39. H. Tagziria, W.D. Hamilton, K. Kumar, J. Phys. G **16**, 1837 (1990).
40. K. Kumar, J.B. Gupta, J. Phys. G **10**, 525 (1984).
41. J.B. Gupta, Phys. Rev. C **29**, 2381 (1984).
42. W.D. Hamilton, K. Kumar, J. Phys. G **5**, 1567 (1979).
43. K. Kumar, J.B. Gupta, Nucl. Phys. A **304**, 295 (1978).
44. B.K. Agrawal, T. Sil, S.K. Samaddar, Phys. Rev. C **63**, 047304 (2001).
45. G.A. Lalazissis, M.M. Sharma, P. Ring, Nucl. Phys. A **597**, 35 (1996).
46. W. Nazarewicz, *Proceedings of the International Conference on Nuclear Structure of the Nineties, Oak Ridge, Tennessee*, Vol. **1** (Elsevier Science Publishers B.V., North-Holland, 1990) p. 60.
47. V. Blum *et al.*, Phys. Lett. B **223**, 123 (1989).
48. V. Blum *et al.*, GSI-88-1, 120 (1988).
49. B. Nerlo-Pomorska, Z. Phys. A **328**, 11 (1987).
50. J. Frana, Acta Polytech. **3**, 127 (1998).
51. R.B. Firestone, V.S. Shirley (Editors), *Table of Isotopes*, 8th edition, 1998 update (J. Wiley and Sons, New York, 1998).
52. R.G. Helmer, H. Debertin, *Gamma and X-ray Spectroscopy with Semiconductor Detectors* (North-Holland, 1989).
53. J. Adam *et al.*, in *Proceedings of the 48th Meeting on Nuclear Spectroscopy and Structure of Atomic Nuclei, Moscow, 16-19 June* (PINP, St. Petersburg, 1998) p. 318.
54. K.Ya. Gromov *et al.*, Nucl. Phys. A **99**, 585 (1967).
55. F. Rossel, At. Data Nucl. Data Tables **21**, 290 (1978).
56. J. Adam *et al.*, JINR Communication, Dubna, P6-86-394, 1986.
57. J. Adam *et al.*, Preprint JINR E6-2001-93, Dubna.
58. R.S. Hager, E.C. Seltser, Nucl. Data Tables A **6**, 1 (1969).
59. D.A. Bell *et al.*, Can. J. Phys. **48**, 2542 (1970).
60. J. Kantele, Preprint RR18/81, University of Jyväskylä, 1981.
61. C.A. Kalfas *et al.*, Nucl. Phys. A **196**, 615 (1972).
62. K. Heyde, R.A. Meyer, Phys. Rev. C **37**, 2170 (1988).
63. J. Adam *et al.*, Preprint JINR E6-2001-154, Dubna.
64. K.S. Krane, Nucl. Instrum. Methods **98**, 205 (1972).
65. D. Venos, private communication.
66. H.W. Taylor *et al.*, Nucl. Data Tables A **9**, 1 (1971).
67. B.S. Dzhelepov, L.N. Zyryanova, Yu.P. Suslov, *Beta Processes, Functions for the Analysis of Beta-Spectra and Electron Capture* (Nauka, Leningrad, 1972).
68. W. Bambynek *et al.*, Rev. Mod. Phys. **1**, 49 (1977).
69. R.A. Meyer, Phys. Rev. **170**, 4 (1968).
70. D.R. Zolnowski *et al.*, Phys. Lett. B **55**, 453 (1975).
71. M. Nomura, Phys. Lett. B **55**, 357 (1975).
72. A. Bohr, B.R. Mottelson, *Nuclear Structure* (W.A. Benjamin, Inc., New York, 1969).
73. H. Ejiri, J. Phys. Soc. Jpn. **24**, 1181 (1968).
74. Y. Varshney, Prog. Theor. Phys. **40**, (1968).
75. S.M. Harris, Phys. Rev. Lett. **13**, 663 (1964); Phys. Rev. B **138**, 509 (1965).
76. M.A. Mariscotti, Phys. Rev. **178**, 1864 (1969); Phys. Rev. Lett. **24**, 1242 (1970).
77. G. Scharff-Goldhaber, C. Dover, A. Goodman, Annu. Rev. Nucl. Sci. **26**, 239 (1976).
78. R.M. Diamond, Phys. Lett. **11**, 315 (1964).
79. D.R. Inglis, Phys. Rev. **96**, 1059 (1954).
80. S.M. Abecasis, E.S. Hernsnoler, Nucl. Phys. A **180**, 485 (1972).
81. R.B. Begzhanov, V.M. Bilenkii, E.I. Volmianskii, Izv. Akad. Nauk SSSR, Ser. Fiz. **43**, 2327 (1979).
82. J. Adam *et al.*, Preprint JINR E6-2002-11, Dubna.
83. R.V. Jolos, Yad. Fiz. **64**, 520 (2001).
84. N. Pietralla, T. Mizusaki, P. von Brentano, Phys. Rev. C **57**, 150 (1998).
85. R.V. Jolos *et al.*, Nucl. Phys. A **618**, 126 (1997).
86. Yu.V. Palchikov, P. von Brentano, R.V. Jolos, Phys. Rev. C **57**, 3026 (1998).
87. F. Iachello, Phys. Rev. Lett. **85**, 3580 (2000).
88. F. Iachello, Phys. Rev. Lett. **87** 052502-1 (2001).
89. P.D. Duval, B.R. Barrett, Nucl. Phys. A **376** 213 (1982).